PROCESSING AND PROPERTIES OF MONOLITHIC INVAR AND COPPER-INVAR-COPPER LAMINATED STRIPS VIA POWDER METALLURGY ROUTE

A Thesis Submitted
in Partial Fulfilment of the Requirements
for the Degree of
MASTER OF TECHNOLOGY

by

SHIVAJI DATTA

to the

DEPARTMENT OF MATERIALS & METALLURGICAL ENGINEERING
INDIAN INSTITUTE OF TECHNOLOGY KANPUR

March,1997

Dedicated

To

Ma and Bapi

CERTIFICATE

This is to certify that the work contained in the thesis entitled *Processing and properties of monolithic Invar and Copper-Invar-Copper laminated strips via Powder Metallurgy route* by *Shivaji Datta*, has been carried out under my supervision and that this work has not been submitted elsewhere for a degree.

R.K. DUBE
Professor
Department of Materials &
Metallurgical Engineering
I.I.T., Kanpur

March, 1997

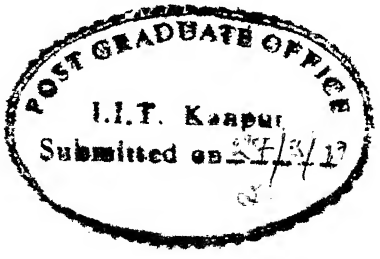

ABSTRACT

The PM processing of speciality thin metal strips is attractive over the conventional strip processing routes considering its potential to the betterment of some properties by maintaining a very high purity and precise composition control in the final alloy. One such speciality strip application is the Copper-Invar-Copper laminated strip of $\sim$ 1 - 2 mm thickness, used as the 'heat sink' in the printed circuit board which warrants matching coefficient of thermal expansion (CTE) with that of the ceramic substrates. The strip is generally manufactured through the conventional roll bonding route. In the present study an effort has been made to prepare the strip through the PM slurry route. Monolithic Invar strip was also prepared through the same route. Mechanically alloyed Invar powder was used in the present study. The PM slurry route consisting of slurry casting (tape casting)$\rightarrow$ sintering $\rightarrow$ hot densification rolling was successfully employed to prepare both the monolithic and laminated strips of $\sim$ 1 mm thickness. The evolution of a sound metallurgical bond between the copper and the Invar layer was studied at various percentages of hot densification rolling with the help of microscopic and EMPA studies. The tensile and 0.2% proof strength of the finished monolithic Invar strip was found to be higher than that achieved in the conventional route because of the contamination of finely dispersed tungsten carbide particles in the Invar matrix which came from the worn out tungsten carbide balls used during mechanical alloying. The CTE values of the monolithic Invar and Cu-Invar-Cu laminated strips were found to be satisfactory. The PM slurry route is capable of tailoring the CTE of the composite strip according to requirement by varying the Cu : Invar : Cu thickness ratio in the finished strip.

ACKNOWLEDGEMENTS

At the very outset I want to express my deep regard and gratitude to my thesis supervisor Dr.R.K. Dube whose brilliant technical prowess and hearty cooperation encouraged me a lot to overcome the frustrated and sluggish moments of experimental research. I would ever remember the unforgettable moments of working with him when he literally guided me through the complicated technicalities of the present work.

I convey my heartfelt thanks to all my friends and seniors who gave their invaluable moral support and companionship to make my stay in the IIT a pleasant experience. Special mention is due to Vinod Narang and Subbrahmanya whose refreshing presence nourished me intellectually.

I am grateful to Dr.V.K. Manglik, Mr.R. Waghmare and Mr.A.K. Shah of the QAMD, Space Application Centre (ISRO), Ahmedabad for allowing me to use the CTE measuring facility and letting me enjoy their hospitality there. Special thanks are due to Mr.A.K. Shah who notwithstanding his packed working schedule took serious interest in my trivial effort.

I am thankful to Mr.S.C. Soni, Mr.P.K. Paul, Mr.R.P. Singh, Mr. Umashankar and Mr.B.K. Jain without whose active cooperation this effort would not have been successful. Thanks are due to the staff members of the Engineering Metallurgy Lab. who selflessly extended their kind cooperation to me during the experimental work.

Finally I want to thank all that silent community who contributed to my effort but might have escaped the glare of my mentioning torchlight and I implore them to pardon me for this unpardonable failing of my memory.

SHIVAJI DATTA

Contents

List of Tables

List of Figures

Chapter 1

INTRODUCTION

Thin metal strips are conventionally manufactured through the ingot metallurgy route which consists of static casting of an ingot or slab, followed by substantial amount of hot and cold rolling. The modern and more efficient method is to cast slab continuously followed by hot and cold rolling. There is an alternative process route available which is not as extensively followed as the conventional route. This alternative process route uses metal powders as the starting material and therefore widely known as Powder Metallurgy (PM) route. The PM route consists of preparing a metal powder preform, followed by sintering and compacting to full density through various means. Eventhough a very small fraction of the global monolithic sheet metal production at present is produced through PM route, it offers attractive prospects in the field of speciality strip manufacturing. There are several PM routes available for the manufacturing of thin metal strips. The most common and extensively followed routes are based on the roll compaction of loose metal powders and rolling of bonded metal powders [1]. These processes have great potential for making multi-layer metal strips as well.

One specific example of multi-layer metal strip is the Copper-Invar-Copper laminated strip, commonly known as copper clad Invar or CCI strip. These copper clad Invar strips find application in the electronic packages as the expansion restraint for the Printed Circuit Board (PCB) structures which doubles as the heat sink due to the good thermal conductivity offered by the outer copper layers of the composite strips. Invar, an alloy of 64 wt% iron and 36 wt% nickel, is extensively used in the precision metrological and cryogenic applications for its extremely low coefficient of thermal expansion (CTE). Of late roll bonded copper clad Invar strips have become important for application in electronic

packages, used in both military and commercial applications, to effect efficient thermal management in them [2].

The Invar and copper clad Invar (CCI) strips prepared through conventional route suffers from unwanted impurity contents such as oxides, sulfur, chromium, manganese, silicon, carbon, etc. which in turn adversely affect the physical and mechanical properties of the strips. But, these strips could very well be processed through the PM route, since for quite some time nickel based magnatic and controlled expansion alloys are made through this route achieving ultra high purity and precise alloy compositions in them [3]. The PM processing of multi-layer strips offers good clad interface between dissimilar metals and the process has the potential to be made automated provided that substantial amount of research and development takes place in this field which is presently very much lacking in comprehensive R&D.

In the ensuing parts of the thesis, Chapter-2 deals with the general aspects of PM processing of metal strips and the different attributes of Invar, Chapter-3 gives the scope and the process outline of the present study, Chapter-4 and Chapter-5 discuss the experimental procedure and the results obtained in the present study respectively, while Chapter-6 lists the conclusions derived from the results and Chapter-7 narrates the suggestions for the future work.

Chapter 2

LITERATURE REVIEW

2.1 PM Processing of Metal Strips

Of late PM processing of metal strips has gained substantial amount of importance due to some advantages offered by it over the conventional route [4]. Among all the PM routes, processing involving roll compaction of metal powders is the most common and commercially attractive process for thin strip production. The roll compaction process has several variations and Dube [1] broadly classified them into the following categories,

1. Routes based on the roll compaction of,
   (a) cold metal powder.
   (b) bonded metal powder in the form of a coherent strip.
   (c) hot metal powder.
2. Routes based on the roll compaction of metal particles other than powder, e.g. compacted strip process.
3. Routes based on the consolidation procesing integrated with the powder production process e.g. spray rolling, direct steel process, direct strip process etc.

In view of the multi-layer strip preparation the PM routes involving roll compaction of (a) cold metal powder i.e. direct metal powder rolling and (b) bonded metal powder in the form of a coherent strip have become attractive. These two processing routes are discussed in the next section. The PM processing based on rolling of metal powders consists of the following unit operations;

1. Preparation of 'green' strip from metal powder.

2. Sintering of the green strip.

3. Densification rolling of the sintered strip.

4. Final cold rolling and annealing.

The first unit operation of 'green' strip preparation from metal powders can be carried out in two different ways - (1) direct metal powder rolling and (2) bonded metal powder rolling.

2.1.1 Direct Metal Powder Rolling

In this process a coherent self-supporting green strip is produced by supplying cold metal powder into the roll gap of a specially designed powder rolling mill which is usually of 2-high type but could very well be of 4-high type. The powder supply could either be horizontal or vertical, while the latter is preferred to avoid the difficulty of feeding loose powder in to the roll gap. There exists two basic methods of feeding metal powder into the roll gap, namely saturated and unsaturated feed systems [5]. In saturated feeding system an excess amount of powder is fed to the nip of the rolls where the frictional forces in between the powders, and the powders and the rolls and the flow properties of the powder determine the total flow of the powder to the roll gap. The powder head in the feed hopper determines the quality of the green strip after roll compaction. In the unsaturated feeding system, a metering device is used in the feed hopper to regulate the amount of powder being fed which generates considerable amount of control difficulties in direct powder rolling. Now a combination of the two, which is known as 'forced feeding' is usually followed to obtain acceptable strip quality. The mechanisms of roll compaction have been studied by many workers [6, 7, 8].

An interesting application of direct powder rolling in making trimetallic multi-layer strip is described by Dustoor [9]. A low cost steel backed aluminium base bearing strip was prepared following direct powder rolling which consisted of preparing an aluminium base bearing layer sandwiched between two surface layers i.e. trimetallic green strip by a powder rolling technique shown in Fig.2.1. The aluminium base bearing layer was made from atomized alloy powder having a composition of Al-8.5Pb-4Si- 1.5Sn-1Cu, which had

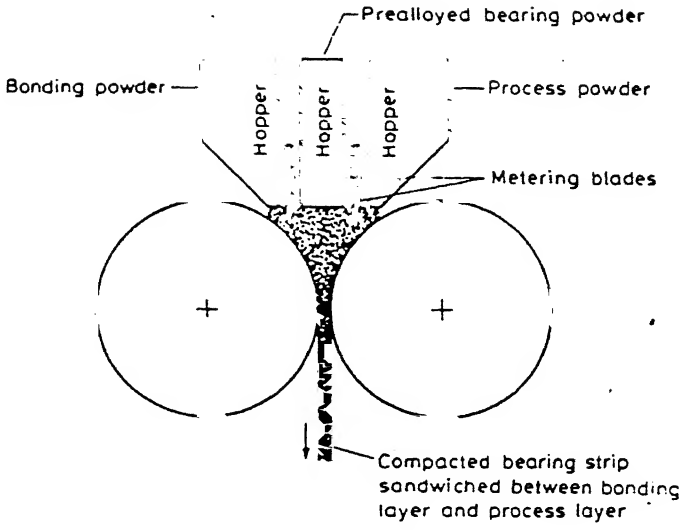

Figure 2.1: Typical arrangement for rolling trimetallic strip (Ref.10)

immiscible lead in finely dispersed state in the alloy powders. The surface layer on one side of the bearing layer was of pure aluminium powder which allows easy cladding to a mild steel strip back-up and the other surface layer was of a metal powder which acted as a sacrificial layer ('process powder') which helps in separaton of the alloy strip from the rolls of the powder rolling mill. The process powder layer was machined off in subsequent bearing finishing operations. The rolling process provided sufficient shear and deformation of each powder prticle due to which a strong green strip resulted from the process. This practice was followed by Imperial Clevite Inc. Technology Centre in Cleveland, Ohio, USA. According to Ro and Toaz [10] it was possible to produce 100% dense green strip which was subsequently sintered at 813K in coil form to enhance strength and ductility of the strip. But there lies a difficulty in the form of variation in density across the thickness of the rolled green strip which could probably be attributed to the different deformation behaviours of powders of the various layers in the strip. In a fascinating study on the rolling of trimetallic Cu-Fe-Cu green strip, Katrus and Vinogradov [11] observed that the outside copper layers became more dense than the core iron layer under the same pressure indicating different deformation behaviour of copper and iron in the trimetallic strip. Direct powder rolling is also used to produce porous nickel strips, used in alkaline battery and fuel cell electodes, by using a spacing agent such as methyl cellulose powder

in the feeding mix prior to the roll compaction [9, 11, 12, 13].

2.1.2 Bonded Metal Powder Rolling

In this process bonded metal powder is fed into the roll gap in the form of a flexible coherent strip. This enables the feeding of accurate amount of powder into the rolling mill which is difficult to achieve in direct powder rolling technique. The preparation of green strip by this method consists of the following basic steps as described by Dube [14],

1. Preparation of a slurry mixture from metal powder, a binder, a solvent medium and a plasticizer depending on the nature of binder.

2. Deposition of the slurry on a substrate.

3. Drying of the slurry on the substrate which after removal from the substrate yields a coherent and flexible 'green' strip.

4. Densification of dried strip by roll compaction followed by other operations like sintering, rolling, annealing etc.

Since the major importance is given to the process of the slurry preparation, this is also known as 'slurry technique' which has some similarity with the powder injection moulding (PIM) process in terms of the slurry chemistry and mixing operations which very much depend upon the proper selection of binder, solvent and plasticizer.

2.1.2.1 Binder

The binder is a temporary vehicle for homogeneously packing the powder into the desired shape and then holding the particles in that shape until the beginning of sintering. The binders are dissolved molecularly in a solvent or are dispersed in a liquid medium as an emulsion. Binder formulations strongly affect the rheology of the liquid phase as in the case of organic binders which increase the viscosity of the solvent and changes the flow characteristic from Newtonian to pseudoplastic in most cases. Generally binders should possess the following attributes [15],

1. Flow characteristics	Viscosity below 10 pa.s at the mixing temperature.
	Strong and rigid after cooling.

	Small molecules to fit between powder particles.
2. Powder interaction	Low contact angle and good adhesion with powder.
	Capillary action of particles.
	Chemically passive with respect to powders.
3. Debinding	Non-corrosive, non-toxic decomposition product.
	Low ash content, low metallic content.
	Easy decomposition at sintering temperatures.
4. Manufacturing	Low cost and easy availability.
	High lubricity for easy roll compaction.
	High strength and stiffness.
	Solubility in common solvents.

Some example binders are paraffin wax, epoxy resin, methyl cellulose, polyvinyl alcohol etc.

2.1.2.2 Solvent Medium

A solvent is used to form the binder soluton. It should have low boiling point, low viscosity, ability to dissolve binder and plasticizer, passivity towards metal powders, non-toxicity, low cost and easy availability. Water is widely used as a solvent medium because it meets most of the attributes quite satisfactorily.

2.1.2.3 Plasticizer

Plasticizers are additives which softens the binder in the dry or partly dry state. These are lower molecular weight organic compounds which dissolve in the same solvent medium as the binder does. This helps in disrupting the close affinity and bonding of the binder molecules thereby increasing the flexibility of the green strip [16]. The most effective additives contain polar anchor groups with a high dielectric character that are strongly attached to the powder surface. The balance of the additive molecule should also be soluble in the binder [15]. Some example plasticizers are glycerol, stearic acid, butyl stearate etc.

2.1.2.4 Slurry Making and Tape Casting

The slurry is made with metal powder, binder, plasticizer and solvent medium keeping the final viscosity in the range of 1 to 1000 Pa.s which makes the slurry substantially homogeneous over a period of time. Thixotropic behaviour arises if too high a solids content is used and the process is sensitive to small variations in temperature and solids content [17]. So a slurry composition is optimized by practice keeping in mind the demands for a particular system. Generally the constituents of a slurry are mixed slowly to avoid air bubble entrapment. To get rid of the adsorbed gases the slurry is transferred to a chamber maintained under vacuum.

After removing the entrapped and adsorbed gases through evacuation technique the mixture is poured into a mould or a substrate with the help of a doctor blade mechanism to maintain the uniformity of the slurry thickness. This doctor blade assisted slurry casting process is also known as 'tape casting' and is widely followed in industry since it is useful for continuous processing [17]. The cast 'tape' is dried in the next step to remove the excess solvent and impart strength to the 'green' tape through gelling reaction in some water based systems. The dried tape/strip is subsequently roll compacted. In one investigation a 1.75 mm thick copper strip was roll compacted to about 70% thickness reduction resulting in a density of 80% of the theoretical value [18].

2.1.3 Sintering

Sintering is the bonding together of particles when heated to high temperatures. On a microstructural scale this bonding occurs as cohesive necks (weld bonds) grow at the points of contact between particles. The roll compacted strip containing 15-20% porosity is low in strength and ductility, which is sintered at suitable temperature to improve physical and mechanical properties. Sintered strips, due to good bonding between the particles caused by neck growth, possess sufficient strength and ductility and is capable of withstanding the handling involved in the subsequent operations. Sintering also removes undesirable impurities e.g. surface oxide films and sulfur from the powder mass provided a suitable sintering atmosphere is used. The suitable atmosphere protects the green strip from oxidation which takes place on the surface as well as in the interior portions of the strip due to interconnected porosity. Generally a reducing atmosphere of either dry H_2 or cracked NH_3 is provided during sintering for a large number of systems. Inert gas

atmospheres like N_2 and argon are another popular choice because of their non reactive nature. Sometimes sintering in vacuum is also carried out as it is clean, reproducible and relatively easy to control. This helps to avoid a low partial pressure of oxygen which can lead to oxide reduction for many metals.

2.1.4 Post-Sintering Densification Techniques

The strip obtained after sintering is quite porous though some amount of densification occurs in sintering which gets reflected in the improved strength and ductility properties of the strip. To achieve full density in the strips they are subjected to post-sintering densification processes which can be classified into two broad categories - (1) repeated cold rolling and sintering/annealing cycle and (2) hot rolling [19].

2.1.4.1 Repeated Cold Rolling - Sintering/Annealing Cycle

Many investigators have reported of obtaining fully dense metal strips made from roll compacted and sintered strip by a series of cold rolling and sintering/annealing cycles [20, 21, 22, 23, 24,]. The porosity content in the sintered strip determines the amount of cold rolling required for full densification of the strip. It is reported that this field lacks in extensive systematic studies for detailed understanding of the mechanisms involved in full densification. Hunt and Eborall [21] showed the dependence of the amount of cold rolling reduction between each anneal in a copper system on the initial density achieved in the preceeding anneal, the variation of density across the strip width and whether or not the strip is coiled after rolling. Sturgeon et al [24] studied the effect of cold rolling on the mechanical properties of sintered stainless steel strips which revealed an optimum peak tensile strength with the amount of cold reduction beyond which mechanical properties deteriorate probably due to fragmentaton of inclusions caused by microcracks at the inclusion-matrix interface.

This process route suffers from the disadvantage that it requires several cold rolling and annealing cycles to produce full density strip which impairs its commercial viability.

2.1.4.2 Hot Rolling

Many investigators have proposed hot rolling after sintering as a means of achieving full density in the metal strip [25, 26, 27]. Sintered strips having porosity content as high

as 80% can be hot rolled to full density in a single pass [19]. The advantage offered by this process are that it enables to produce full density strip in a single operation while reducing the sintering time and it is possible to hot roll the sintered strip from the sintering furnace directly after sintering, thereby saving time and energy and offering the possibility of continuous processing. The amount of hot rolling reduction, required to achieve full density in the final strip, is dependent on the initial porosity content of the strip and it is greater than the theoretically required reduction since some amount of rolling deformation goes in elongating the strip instead of closing the pores. The densification in this process results from compaction by rearrangement and restacking of particles in the system under the specified conditions. Some workers [26] have studied the effect of the different amounts of hot rolling reduction on the mechanical properties of the hot rolled strip which showed the interrelation of the initial strip density with the change in mechanical properties in the final strip with varying amounts of hot rolling reduction. Studies [28] have been conducted to find out the possibility of hot rolling the sintered strip direct from the sintering furnace.

The strips hot rolled to full density are either fully cooled in a reducing atmosphere or partially cooled in a reducing atmosphere after water cooling and pickling, which reduces production time.

2.1.5 Final Cold Rolling and Annealing

The PM strips produced through the hot rolling route are sometimes given a certain amount of cold reduction and annealed before despatch, while the strips produced through the repeated cold rolling and sintering/annealing cycle route are invariably given a final annealing treatment according to the requirement before despatch. This is done to achieve better surface property along with better and homogeneous overall strip properties.

2.2 Invar - The Iron-Nickel Alloy of Low Thermal Expansion Coefficient

2.2.1 Historical Background

The very low thermal expansion of the Fe-36Ni alloy at room temperature was discovered way back in 1896 by the famous metrologist C.E.Guillaume and it was properly named 'Invar' due to its almost negligible amount of change in linear dimensions in a certain range of temperature. Presently the class of Fe-Ni alloys having Ni content in the vicinity of 36 wt.% is known as the 'Invar family of alloys'. Of this family two alloys are extensively used - one is Fe-36Ni alloy, the classical low expasion alloy, used mostly in metrology and electronic packaging applications and the other is Fe-42Ni alloy, used in electrical and electronic industry, especially in the glass to metal seal applications since its coefficient of thermal expansion (CTE) closely matches with that of the silicate glasses. Eventhough the last year (1996) saw the centenary celebration of the discovery of Invar still a lot of research is going on in this wonder alloy, since the reason of its unique property is not yet fully understood and fundamental reaserch is needed to meet the challenges created by its application in the field of cryogenic engineering and electronic packaging which is advancing rapidly with the astronomical proliferation of information technology.

2.2.2 Invar Effect and Magnetostriction

The Invar alloy of 64Fe-36Ni composition has a minimum CTE of about 1.2 $\times 10^{-6}$/K which is almost constant over the temperature range of 173K to 473K. This expansion anomaly, popularly known as the 'Invar effect', is pronounced only below the Curie Point (T_c) which is close to 555K for Invar, beyond this temperature CTE reverts to normal condition i.e. it shows rapid increasing trend. The other alloys of Invar family having higher Ni content have low average CTE spread over a wider temperature range. But the 36Ni Invar maintains its low CTE down to absolute zero temperature making it an obvious choice for application in cryogenics [3].

The anomalous thermal expansion behaviour or for that matter 'Invar effect' is associated with the magnetic properties of the alloy, the low expansion being a balance between

normal thermal expansion and contraction due to 'magnetostriction', a phenomenon defined as the change in linear dimensions of a body resulting from magnetization which is also known as 'Joule effect' [29]. Nakamura [30] described that the anomalous expansion behaviour occurs just below the T_c of the alloys and therefore in the ferromagnetic phase when the temperature falls through the T_c while cooling, the structure changes from the paramagnetic state, in which the magnetic moments of the atoms are disordered, to the ferromagnetic state, where they become aligned. This transformation is accompanied by a change in volume caused by the ferromagnetic coupling of the moments (parallel spins), corresponding to the spontaneous volume magnetostriction. This change in volume due to the onset of ferromagnetism is superimposed on the natural variation due to the change in amplitude of thermal atomic vibrations as the temperature decreases, thus causing net low volume change with change in temperature. During heating also the same sequence of events take place upto the temperature T_c giving rise to very low CTE of the material, beyond T_c the ferromagneic state changes to the paramagnetic state causing rapid change in CTE with temperature. The 'Invar effect' and 'magnetostriction' are discussed in detail by E. du Trémolet de Lacheisserie [30].

2.2.3 Effect of Different Elements on The Properties of Invar

The success of the Fe-Ni alloys especially Invar, is due to the particular physical properties, which are determined essentially by the concentration of the major alloying elements as well as by the amount of minor and trace elements present in the alloys. The Fe-Ni binary phase diagram is shown in Fig.2.2.

2.2.3.1 Effect of Alloying Additions

The remarkable low thermal expansion property of Invar mesmerized the scientific community all over the world on its discovery, but it was subsequently found out that the CTE changes with time at room temperature. This ageing phenomenon is largely dependent on the alloying elements other than Fe and Ni. The effect of the variation of Ni content in Fe-Ni alloy on the CTE value is shown in Fig.2.3.

In general the effects of such alloying elements in Fe-Ni alloy are twofold. Firstly, they increase the minimum value of CTE of the alloy and secondly, they modify the Ni content corresponding to this minimum value. This is illustrated for C, Cu, Ti, Mn and

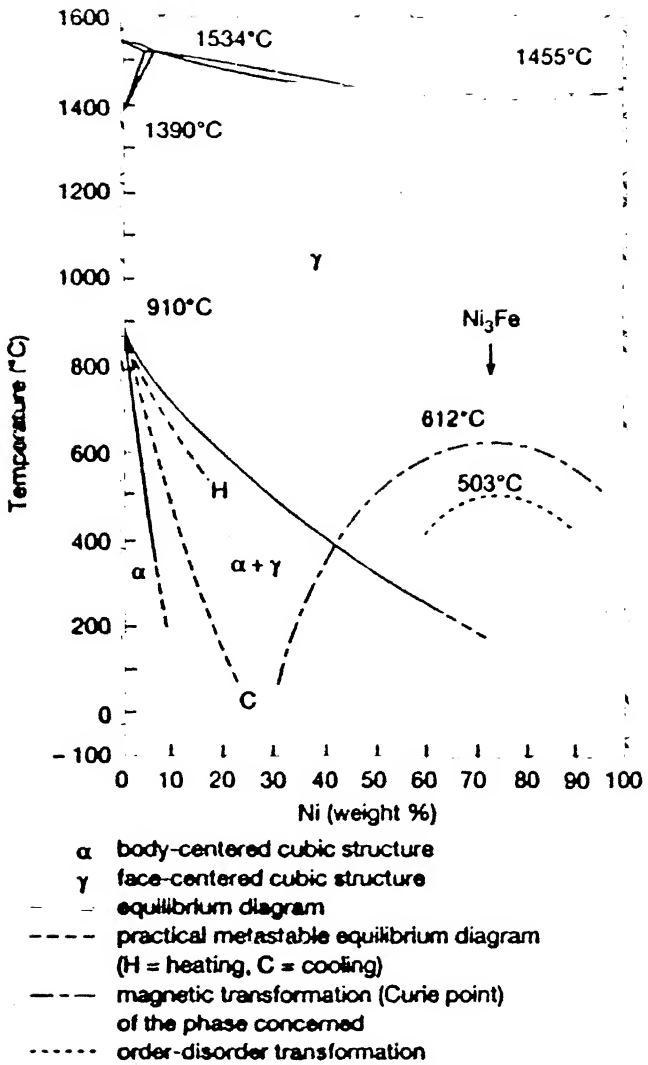

Figure 2.2: Fe-Ni binary phase diagram

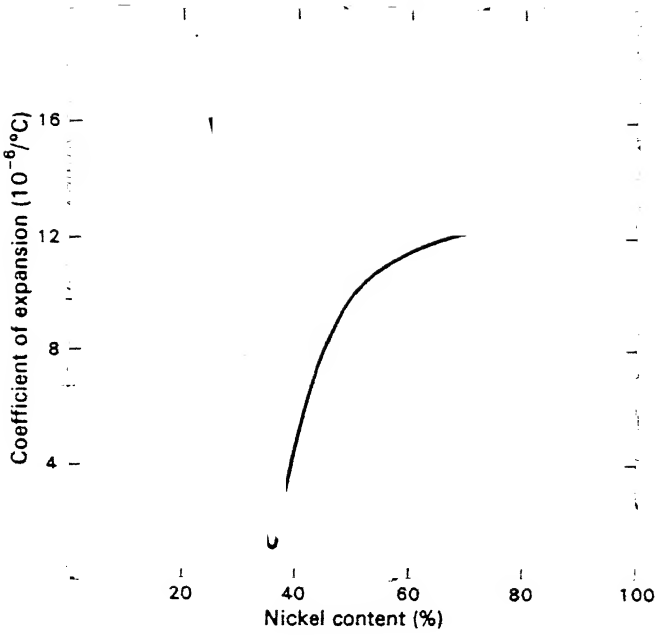

Figure 2.3: Expansion coefficient at 293K of Fe-Ni binary alloys

Table 2.1: Effect of various elements on the mean value of CTE (from 293K to 373K)

Element	Si	Mn	Cr	Cu	Co
change in CTE per % addition ($\times 10^{-6}$/K)	+1.3	+1.0	+0.8	-O.1	0

Cr in Fig.2.4 and 2.5. With the exception of cobalt [29] most common elements raise the minimum value, and the principal conclusion which can be drawn from these studies is the advantage of reducing the levels of residual elements in Invar. Table 2.1 gives the effects of various elements on the average CTE value between 293K and 373K, determined from multiple correlation studies on industrial heats of Invar alloy (64Fe-36Ni) [31].

Elements such as Cr and Cu must be controlled by careful selection of raw materials, while Mn and Si levels can be maintained below about 0.1 wt.% by good deoxidation and desulfurization practice of the Invar melt. With very low residual level of impurities in Invar it is possible to achieve a CTE value close to 0.8 $\times 10^{-6}$/K [31].

In the same way as the CTE, alloying additions modify both the minimum value of the room temperature Young's modulus and Ni concentration at which this minimum value is observed.

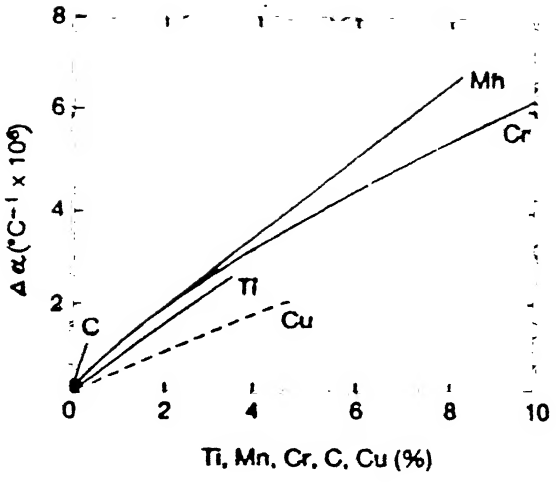

Figure 2.4: Increase in the expansion minimum produced by additions of C, Cu, Ti, Mn and Cr. (Ref. 31)

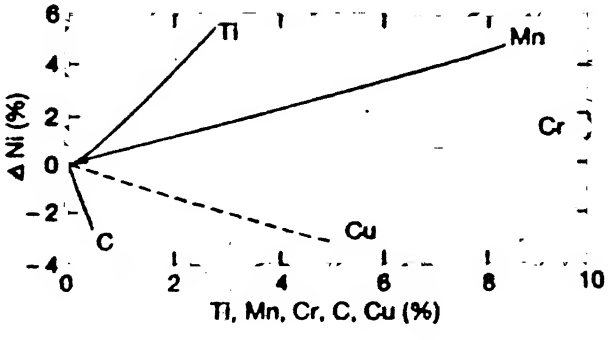

Figure 2.5: Shift in the Ni content corresponding to the expansion minimum produced by additions of C, Cu, Ti, Mn and Cr. (Ref. 31)

Table 2.2: Influence of minor and trace elements on the properties of Fe-Ni alloys

Element	Property (Deterioration)	Property (Improvement)
Hydrogen	Internal soundness	
Nitrogen	Internal soundness	
	Ductility	
Oxygen	Weldability	
	Magnetism	
	Ductility	
	Internal soundness	
	Surface defects	
Sulfur	Workability	Machinability
	Weldability	
Calcium	Weldability	
	Electromagnetism	
Magnesium	Weldability	Workability
	Magnetism	
Aluminium	Ductility	
	Magnetism	
Carbon	Magnetism	
	Thermal expansion	

2.2.3.2 Effect of The Minor and Trace elements

The influence of the minor and trace elements on the properties of Fe-Ni alloys is given in Table 2.2.

Among the trace elements, importance is given to sulfur and oxygen since the complex iteraction among them affects the behaviour of Invar during secondary processing operations, such as chemical and mechanical machining, solidstate refining in H_2 and welding. Invar shows a high temperature ductility loss between 973K to 1273K which increases with increase in sulfur content. According to Ben Mostapha et al [32], the embrittlement is due to loss in grain boundary strength, related to both the segregation of sulfur and the formation of intergranular precipitates. Generally a common practice is to use solidstate refining processes such as high temperature heat treatment in pure H_2 on thin sections of Invar to get rid of sulfur, carbon and oxygen. Still in the conventional route it is not possible to systematically reduce sulfur level to a minimum and therefore it is often necesssary to seek a trade-off between beneficial and deleterious effects [30].

2.2.4 Effect of Processing Parameters on The CTE of Invar

The physical and mechanical properties of Invar not only get affected by the presence of minor and trace elements in them but also by the processing attributes like amount of cold work, texture etc. The expansivity of fully annealed Invar is appreciatively higher than that of quenched or cold worked material, while quenching and cold working significantly lower the CTE of Invar. With higher amount of controlled cold work, the value of CTE can be reduced to zero or even slightly negative in the case of a Superinvar [31]. But the extremely low CTE values of quenched and cold worked Invar are unstable with respect to time and temperature. This is generally stabilized by subjecting the thin sections to low temperature annealing [29]. In all the annealing operations the furnace atmosphere should be free from sulfur as Invar is susceptible to attack by sulfur and oxygen at elevated temperatures.

2.2.5 Application of Low Expansion Alloys in Electronic Packaging

The heart of an electronic package is the Printed Circuit Board (PCB) on which electronic components such as Integrated Circuits (IC) are packed. The industrial manufacture of ICs and the performance of electronic devices depend strongly upon the development of new materials and processes. In particular, large scale production of ICs was made possible by the use of alloys with CTE matched to that of silicon. The first silicon chips were brazed to the supports made from Fe-29Ni-17Co alloy corresponding to the Kovar grade, a derivative of the Invar family of alloys. Subsequently the Fe-42Ni low expansion alloy supports were introduced as the lead frames for the chip carriers because of its CTE being very close to that of the chip substrate materials like silicon, gallium arsenide etc.

2.2.6 Copper-Invar-Copper Laminated Strip : A New Material for Electronic Packaging Applications

The tiny electronic components mounted on the PCBs suffer from cyclic heating and cooling caused due to the passage of electrical current through them which results in cyclic expansion and contraction. This gives rise to thermal fatigue failure in them. This has serious implication with respect to the smooth functioning of the electronic devices.

One aproach to overcome this problem is to use heat conducting lead frames and 'heat sinks' which also act as an expansion restraint and are also known as 'cold plates'. One very well known heat sink material is Copper-Invar-Copper laminated strips or Copper clad Invar (CCI) strips [2, 33]. The heat sinks are typically adhesively bonded or soldered to the component it supports or placed in between the layers of a multi-layered PCB as is shown in Fig.2.6. The roll bonded thin Cu-Invar-Cu strips are used as heat sinks since the CTE of the laminated strip can be custom-made by varying the thickness ratio of copper to Invar to suit the specific requirement. This combination exploited the high thermal condutivity of copper and the very low CTE of Invar to its advantage.

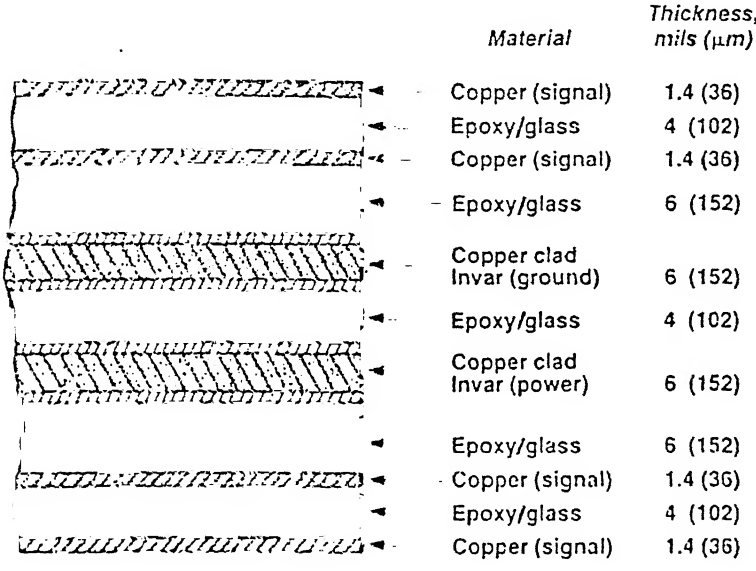

Figure 2.6: Layers of Copper clad Invar foil incorporated in conventional epoxy/glass or polyimide/glass board structures. (Ref. 2)

2.2.7 PM Processing of Monolithic Invar and Copper-Invar-Copper Laminated Strips

Of late the PM processed Invar alloys are attracting a substantial amount of attention from the researchers of many countries due to several advantages offered by PM products. In a recent study in the CIS [34] researchers have tried to judje the 'Invar effect' in powder metallurgy Fe-36Ni alloy by correlating the Poisson's ratio and the CTE. There is a trend

of producing complex components through powder injection moulding (PIM) route. In a recent study [35] investigators have reported successful preparation of wave guides of Fe-36Ni Invar alloy, needed in electronic industry, through the PIM process.

The Copper-Invar-Copper laminated strips are generally produced through the roll bonding route in which the diffusion of Cu to Invar, and Fe and Ni to copper layer take place due to prolonged heating associated with the process. Now large scale diffusion of Cu into Invar can incrase the CTE of Invar which has deleterious effect from the point of view of its intended application requirement. So to prevent this, the PM processing of Copper- Invar-Copper laminated strips can be adopted in which the process route has been manipulated in such a manner that the strips remain at high temperatures for a short time thereby reducing the chances of large scale atomic diffusion at the interface. This will have an added advantage from the point of impurity control and precise composition control in the finished strip which are the typical advantages offered by the PM processing over the conventional strip processing.

Chapter 3

SCOPE & PROCESS OUTLINE OF THE PRESENT STUDY

3.1 Scope

In the present study an attempt has been made to prepare monolithic Invar and Copper-Invar-Copper laminated strips following the PM route of bonded powder rolling. The actual process route followed in the present study is schematically described through the process outline given in Fig.3.1. Slurry casting technique was used to prepare the green monolithic and three-layer laminated strips. Unlike the conventional bonded powder rolling route the green strips were not subjected first to roll compaction, instead they were sintered followed by hot densification rolling to full density.

Keeping in mind, the problems associated with the rolling of the trimetallic green strips involving metal powders having different densification behaviour [11], the following aims were pursued,

1) To study the feasibility of the slurry casting-sintering-hot rolling route for the preparation of monolithic Invar and trimetallic Copper-Invar-Copper strips.

2) To study the diffusion behaviour of the constituent metallic elements along with the microstructural and physical evolution of the Copper-Invar interface at different amounts of hot rolling reduction.

3) To study the mechanical and physical properties of the prepared strips.

3.2 Process Outline

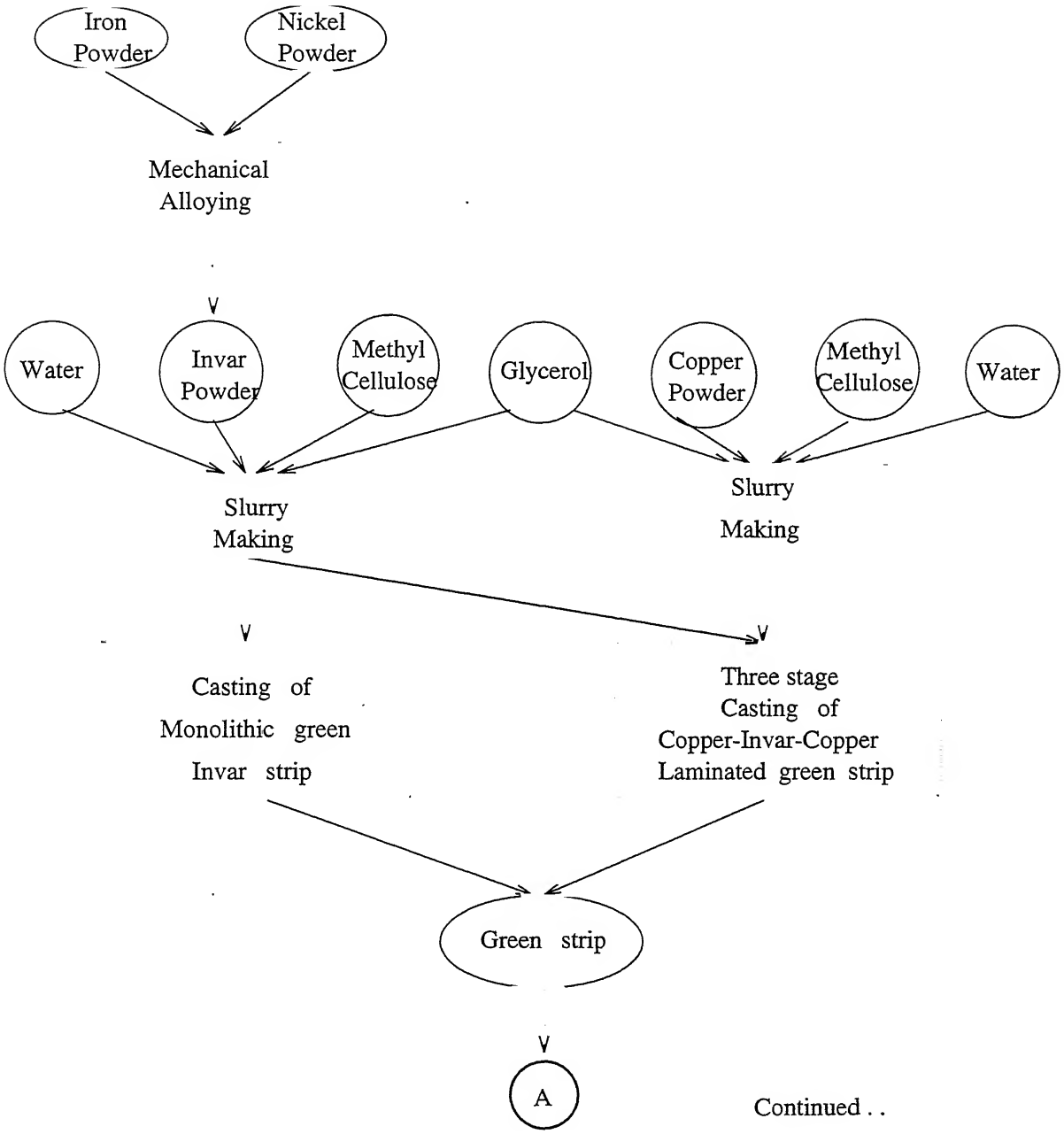

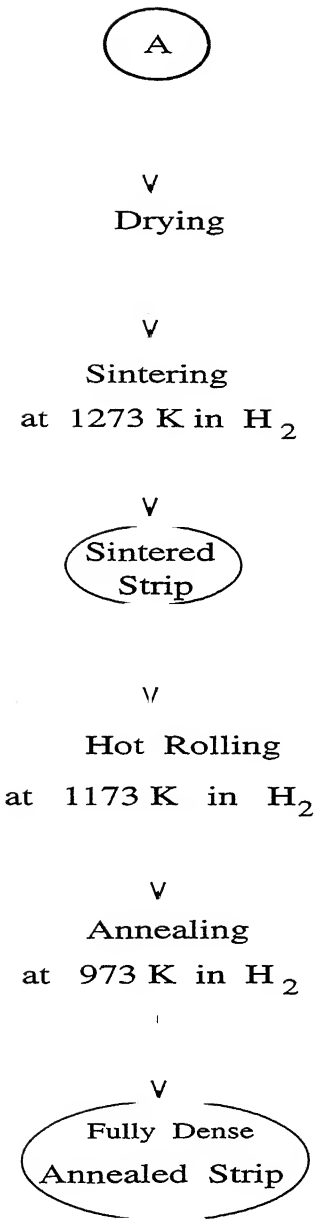

Figure 3.1: Schematic process flow diagram followed in the present study

Chapter 4

EXPERIMENTAL PROCEDURE

4.1 Materials

4.1.1 Iron Powder

Electrolytic iron powder supplied by Sudhakar Products, Bombay was used. The particle size distribution and a typical SEM micrograph of the iron powders are shown in Fig.4.1 and Fig.4.2 respectively.

4.1.2 Nickel Powder

INCO type 123 nickel powder was used. The particle size distribution and a typical SEM micrograph of the nickel powders are shown in Fig.4.3 and Fig.4.4 respectively.

4.1.3 Copper Powder

Atomimized copper powder supplied by Greenback Industries, Inc., U.S.A was used. The particle size distribution and a typical SEM micrograph of the copper powders are shown in Fig.4.5 and Fig.4.6 respectively.

4.1.4 Binder

Reagent grade anhydrous methyl cellulose powder having methoxy content of 28% - 32% was used as binder.

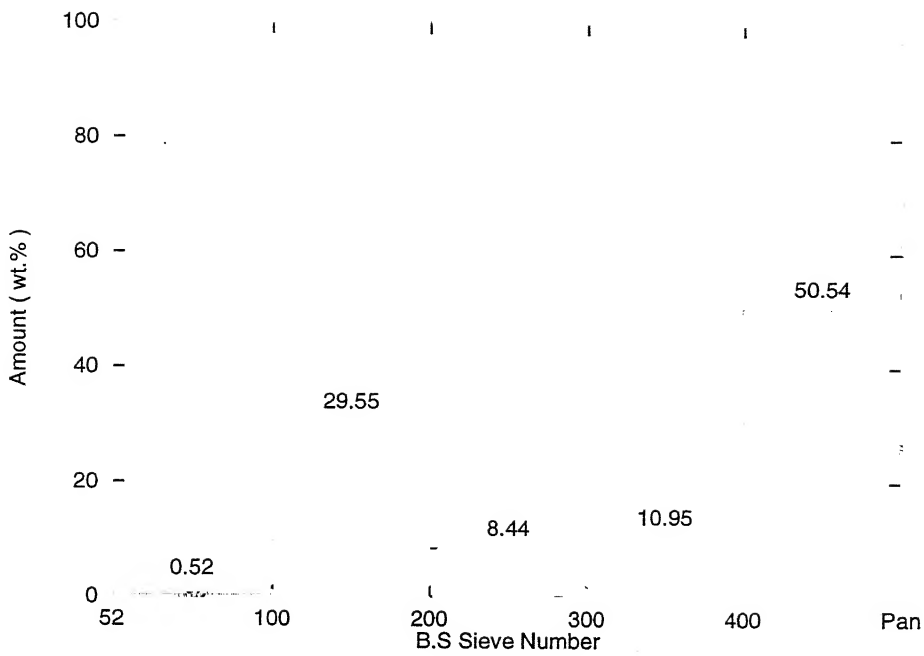

Figure 4.1: Particle size distribution of iron powder

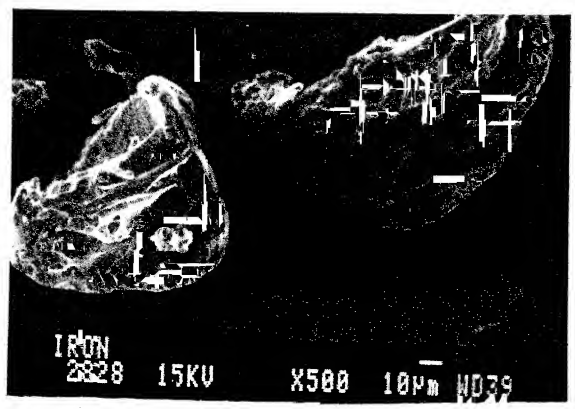

Figure 4.2: SEM photomicrograph of iron powder

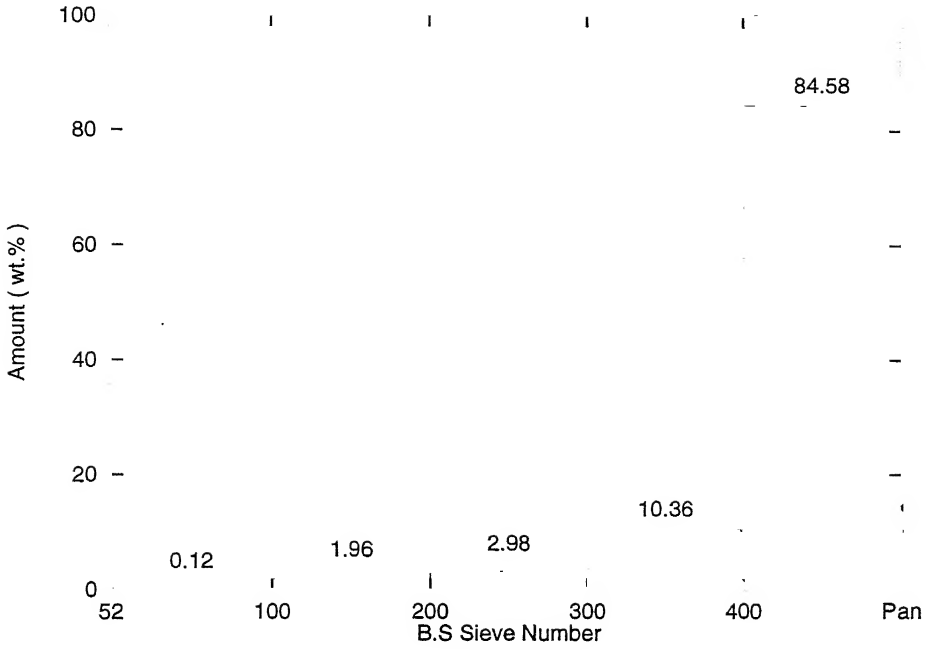

Figure 4.3: Particle size distribution of nickel powder

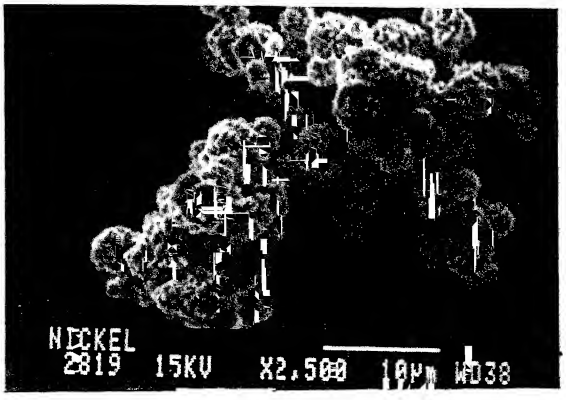

Figure 4.4: SEM photomicrograph of nickel powder

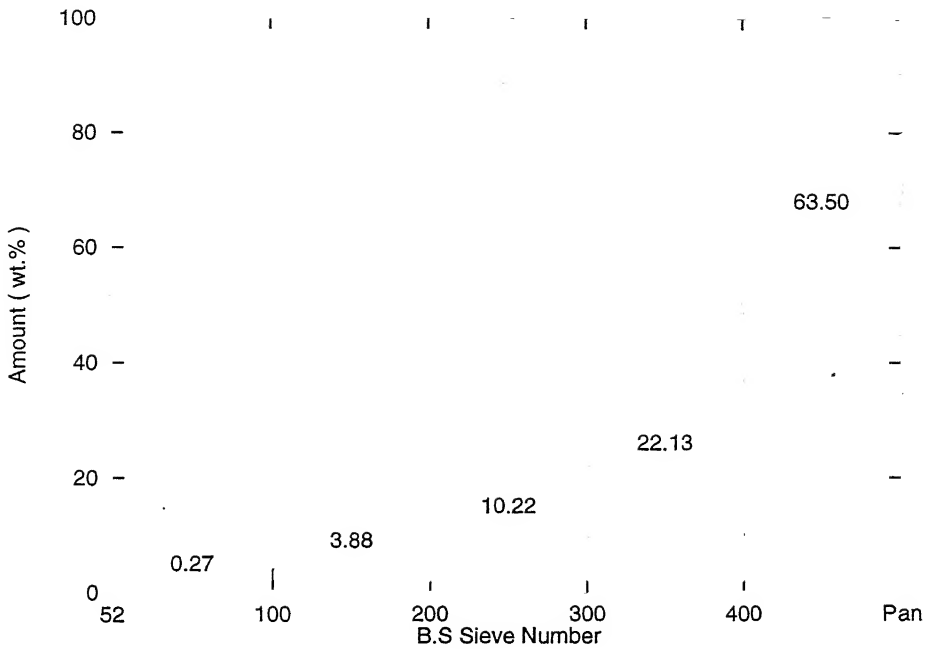

Figure 4.5: Particle size distribution of copper powder

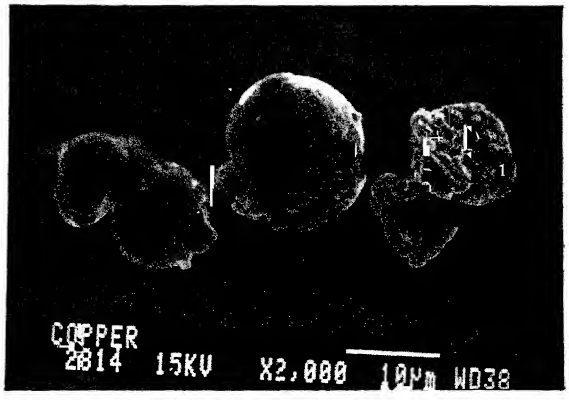

Figure 4.6: SEM photomicrograph of copper powder

4.1.5 Plasticizer

Reagent grade glycerol having density of 1.255 - 1.260 g/ml at 293K and ash content of not more than 0.02% was used as plasticizer.

4.1.6 Vehicle Medium

Distilled water was used as a vehicle medium for the binder solution.

4.1.7 Gases

IOLAR-2 grade argon and hydrogen gases were used in the present work.

4.2 Preparation of Invar Powder

The Invar powder was prepared by mechanical alloying (hitherto mentioned as MA) of high purity iron and nickel powders in a high energy TC Attritor Mill of Torrance make. It had a maximum power rating of 0.74 kW and a provision for water cooling of the milling chamber from outside. Tungsten carbide balls of 3 mm diameter were used as the grinding medium. A powder mix of 64 : 36 ratio by weight of iron and nickel powders respectively was mechanically alloyed in dry condition at the maximum shaft speed of 245 r.p.m in the mill for various periods of time up to a muximum of 32 hours. The milling was carried out in an inert dry argon gas atmosphere using ball to charge ratio of 32 : 1 by weight. The optimum time required for alloying was determined by X-ray diffraction studies carried out on powder samples drawn out from the mill at time intervals of 2 hours, 4 hours, 8 hours, 16 hours, 24 hours and 32 hours of milling.

4.3 Preparation of 'Green' Strips by Slurry Casting Method

The monolithic and laminated 'green' strips were prepared by using the batch process of slurry casting method. Monolithic green strip of Invar was prepared from an Invar slurry and the laminated strip was prepared from the Invar slurry, and a copper slurry was used

Table 4.1: Invar slurry composition

Constituents	Amount
Invar powder	77.17 wt%
Methyl cellulose	0.77 wt%
Glycerol	2.76 wt%
water	19.30 wt%

Table 4.2: Copper slurry composition

Constituents	Amount
Copper powder	69.97 wt%
Methyl cellulose	0.69 wt%
Glycerol	3.67 wt%
water	25.67 wt%

for lamination. The composition of the Invar and copper slurries are shown in Table 4.1 and 4.2 respectively.

At first a dry premix of binder and metal powder was prepared and then a solution of glycerol in water was made. This was done to prevent the agglomeration occurring during direct mixing of binder with solvent. Then the premix was mixed with the aquous solution of glycerol in a beaker with the help of a laboratory stirrer for 10 minutes and a homogeneous slurry having good flow characteristics was obtained. Mixing by the stirrer and casting of the slurry were done slowly and carefully to reduce the amount of entrapped air bubbles in the cast strips.

The monolithic green strip of Invar was prepared by casting the Invar slurry into a single stage flat horizontal detachable type glass mould of size $20mm \times 40mm \times 6mm$. Prior to pouring, the mould was thinly coated with oleic acid which acted as a raleasing agent. After pouring, the excess slurry was scrapped off the mould by a scrapper blade i.e. doctor blade to maintain the uniformity in thickness of the green cast strip. The cast strip in the mould was dried in hot air blast for 5 to 10 minutes.

For the laminated green strip preparation a three stage flat horizontal detachable type glass mould of size $20mm \times 40mm \times h\ mm$ was used in which the height ($h\ mm$) of the mould was progressively built up in three stages as shown in Fig.4.7 (the individual thicknesses of stage-I, stage-II and stage-III were 1.5 mm, 6 mm and 1.5 mm respectively).

In the first step, copper slurry was cast in first stage of the glass mould in a manner followed in casting monolithic Invar strip and it was allowed to dry in hot air blast for 5 to 10 minutes. In the second step, the height of the mould was increased by placing the second stage of the mould, which is a thick hollow glass frame, on top of the first stage of the mould. The Invar slurry was cast in the second stage of the mould on top of the partially dried copper slurry previously cast and allowed to dry for 10 to 15 minutes. In the third and the final step the height of the mould was further increased by placing the third stage of the mould, again a hollow thick glass frame, on top of the second stage of the mould. The copper slurry was cast in the third stage of the mould on top of the partially dried Invar slurry and the resulting composite strip was allowed to dry for 5 to 10 minutes. Thus a three layer laminated green strip was obtained.

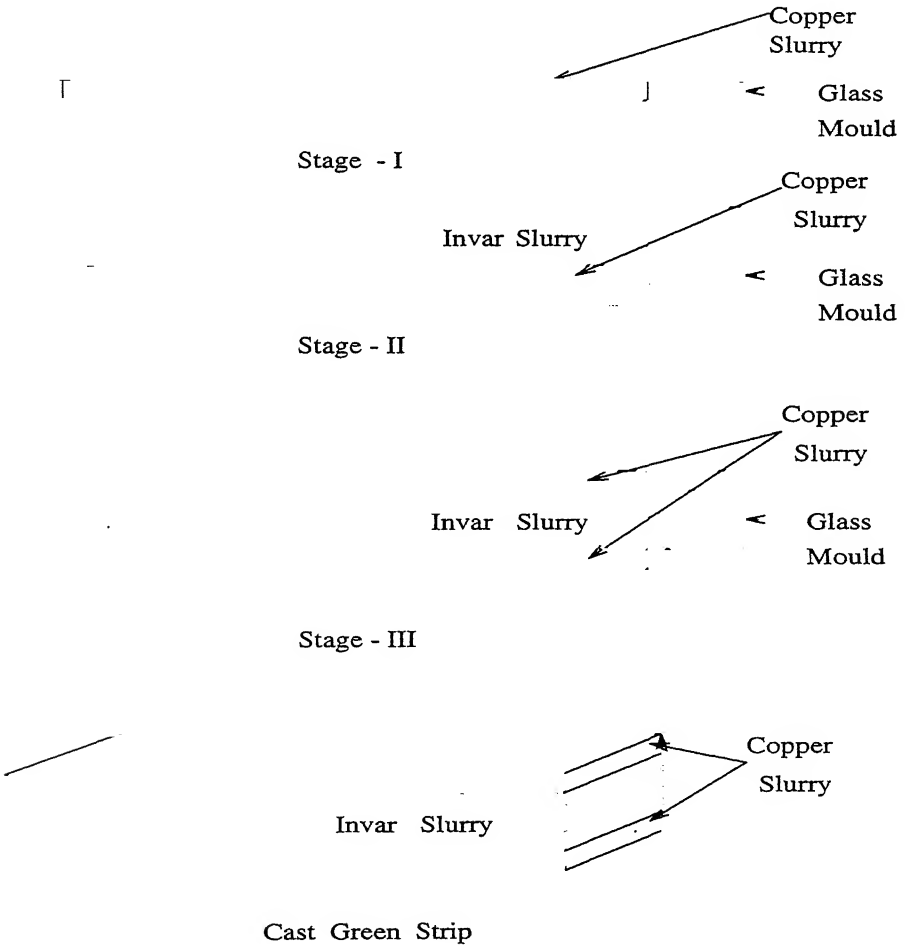

Figure 4.7: Three stage slurry casting process (schematic)

The green strips were dried in a hot air oven at 383K for 2 hours and the dried strips

were subsequently stripped off from the glass mould.

4.4 Sintering of The Green Strips

The green strips were sintered in a specially designed furnace. The heating chamber, which was heated by silicon carbide rods, consisted of an Inconel tube, 750 mm long and of 100 mm internal diameter and was closed from one end. The constant temperature hot zone of size 200 mm existed at the closed end of the furnace. The open end of the furnace had 200 mm. long cooling chamber where the sintered strips were cooled under protective atmosphere. Gases were introduced at the closed end of the chamber through a thin Inconel tube passing through the open end of the chamber.

The dried green strips were sintered at 1273K for 900s in dry H_2 gas atmosphere. After sintering the strips were slowly transfered into the cooling zone of the furnace where they were cooled in H_2 gas atmosphere.

4.5 Hot Densification Rolling of The Sintered Strips

The sintered strips (both monolithic and laminated) were porous and contained about 45% porosity. Therefore in order to make a fully dense strip, these were hot rolled in dry condition. A small hole was drilled near one end of the sintered strip through which a thin nichrome wire was fastened which was required for pulling the hot strip through the rotating rolls during hot rolling opetation. The sintered strips fastened with a nichrome wire were slowly introduced one at a time into the hot zone of a specially designed re-heating furnace interlinked with a 2-high rolling mill. Preheating for each strip was done at 1173K for 600s in dry H_2 atmosphere. Hot rolling was done on a single stand, non-reversing, 2-high rolling mill, having 135 mm diameter rolls, rotating at a fixed speed of 55 r.p.m. The preheating furnace was interlinked with the rolling mill in such a manner that the strips remained in the protective atmosphere upto the roll nip. The set up for the hot rolling of porous sintered strip under protective atmosphere is schematically shown in Fig.4.8. Thickness reduction was achieved by pulling the strip by the wire fastened to it and forcing the hot strip to pass through the rotating rolls set at a pre-determined roll gap. Soon after rolling, the strips were cooled in a bed of fine graphite chips to prevent internal oxidation of the strips caused by the interconnected pores present in it. The

strips behaved well during hot rolling and there was no significant edge cracking after rolling. However, after each rolling pass the cracked portion of the longitudinal edges of the strips were trimmed to avoid growth of these cracks in the subsequent passes. The sintered strips were hot rolled to 24%, 32%, 53%, 66%, 72%, 77%, 83% and 85% thickness reduction. Upto 66% thickness reduction, it was possible to hot roll in a single pass. Beyond it, hot rolling was done in more than one pass.

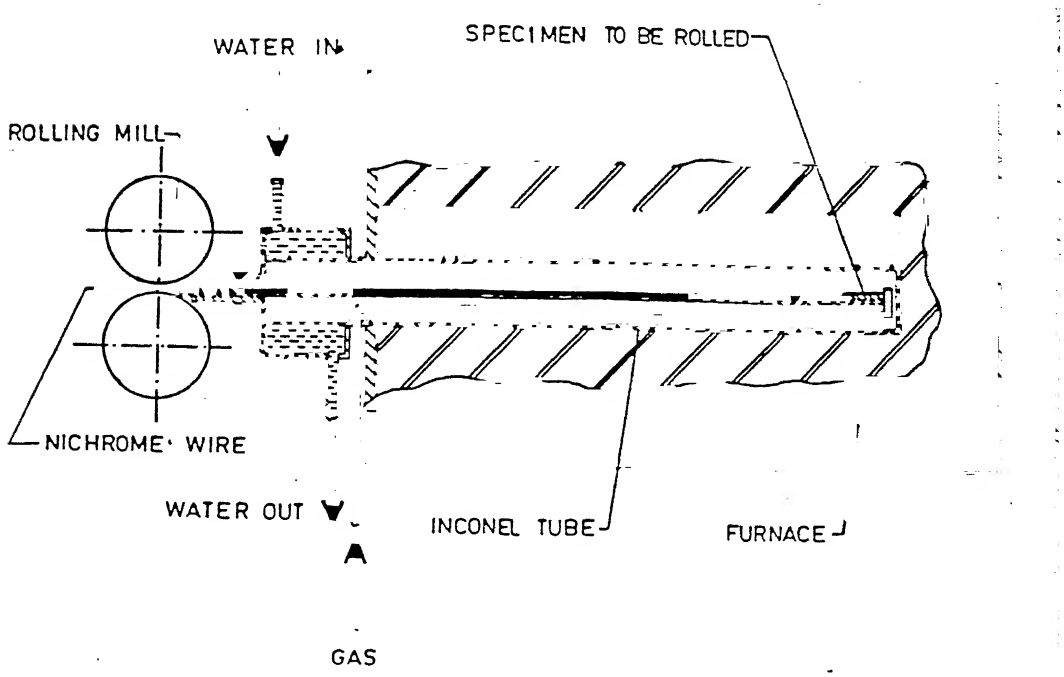

Figure 4.8: Hot rolling arrangement

4.6 Post-Densification Annealing

During hot rolling the hot rolls were not preheated, therefore when hot sintered strips came in contact with the cold rolls, there was a chilling effect, in particular, on the surfaces of the strip. This would bring down the temperature of the surface layers leading to 'warm' working condition. Therefore the densified strips after hot rolling were annealed at 973K in dry H_2 atmosphere for 1800s in the horizontal tube Inconel furnace and cooled in the cooling zone of the furnace under the protective atmosphere.

4.7 Characterization Methods

Mechanically alloyed Invar powder was subjected to X-ray diffraction studies and sieve analysis was carried out for all the metal powders. The sintered, partially densified, fully densified and post-densification annealed strips of Invar and Cu-Invar-Cu were tested for various mechanical and physicl properties.

4.7.1 Sieve Analysis

Different metal powders used in the present study were characterized for particle size distribution by standard sieve analysis technique using the British Standard (B.S) sieves.

4.7.2 X-Ray Diffraction Analysis of The Invar Powder

X-ray diffraction patterns for the MA Invar powder were obatined from the X-ray diffractometer model RICH SIEFERT ISO DEBYEFLEX 2002, Germany. Cu-$K_{i\alpha}$ radiation was used for the X-ray diffraction studies. The optimum time of milling for alloying was determined by matching the obtained diffraction patterns with the ASTM Powder Diffraction File data.

4.7.3 Scanning Electron Microscopy

Different metal powder morphologies and microstructure of sintered, hot rolled and final annealed strips were observed under a JEOL JSM 840A, Scanning Electron Microscope (SEM). The metal powder morphologies were observed dispersing the powders with acetone on finely polished brass stubs prepared especially for this purpose. For observing

the structure and to save the pores from being filled by ductile copper during polishing operations, the sintered and the partially densified strips were first impregnated in vacuum with low viscosity cold setting resin and these were subsequently mounted with cold setting powder and resin. Sample preparation for the microstructural studies consisted of standard emery paper polishing followed by fine cloth polishing with 0.3 μ m alumina abrasive particles in suspension with water. The rolling direction along the thickness of the rolled strips was kept as the direction of observation. Samples were etched with $FeCl_3$ in diluted HCl solution for 20s prior to the observation under the microscope.

4.7.4 Electron Micro Probe Analysis Studies

Electron micro probe analysis (EMPA) studies were carried out to obtain the concentration profile for Cu, Ni and Fe across the Copper-Invar interface in sintered, partially densified, fully densified and post-densification annealed strips. Both qualitative and quantitative studies were done to know the final composition of the invar powder produced through MA for 32 hours. EMPA studies were conducted in a JEOL SUPERPROBE JXA 8600 MX, Electron micro probe analyser. The concentration profiling was done at an interval of 20 μ m on both the sides of the interface perpendicular to the rolling direction.

4.7.5 Microhardness Testing

Microhardness of the rolled Cu-Invar-Cu laminated strips was measured in a LEITZ MINILOAD-2 Microhardness tester for hardness profiling across the Copper-Invar interface. Readings were taken at an interval of 20 μ m on both sides of the interface perpendicular to the rolling direction. 98.01 mN load was applied for the indentation purpose and the hardness was expressed in terms of HV scale of hardness.

4.7.6 Tension Testing

Ultimate tensile strength (UTS), 0.2% proof strength and percent elongation were measured by uniaxial tension testing on an INSTRON-1195 machine. The testing was done at room temperature and at a cross-head speed of 0.5 mm./min. Due to limited amount

of strip material, the specimen used was not of standard specification as per BS 18 specification [36]. However the geometry of the specimen as per above specification was maintained, as shown in Fig.4.9. A minimum of three samples were tested in each case.

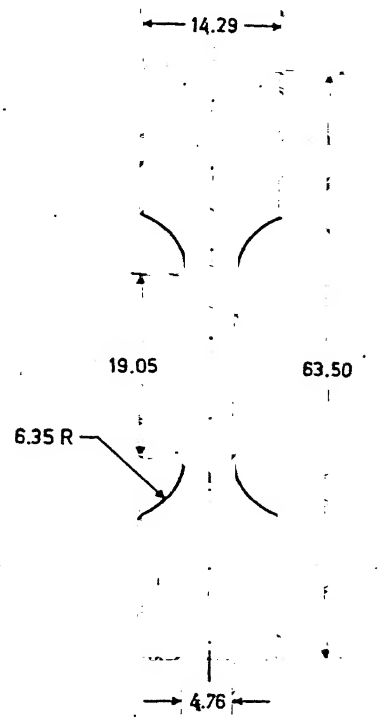

Figure 4.9: Tensile test specimen (units in mm) (Ref.36)

4.7.7 Fractography

The uniaxial tension test fractured surfaces were observed under JEOL JSM 840A Scanning electron microscope.

4.7.8 Density Measurement

Density of the fully dense hot rolled and annealed monolithic invar and Cu-Invar-Cu laminated strips were measured by displacement method using the Archimedes' Principle.

4.7.9 Measurement of Coefficient of Thermal Expansion (CTE)

The coefficient of thermal expansion (CTE) of monolithic Invar and Cu-Invar-Cu laminated strips were measured in a ULVAC-SINKU RIKO DL-1500, Thermal Dilatometer.

This device is used for the measuring and recording of changes in length of solids with change in temperature. The principle of this thermal dilatometer is based on the method commonly called the 'pushing rod method'. The sample was put into a vertical tube in such a way that one end was parallel to the measuring movement. A push rod, made of the same material as the sample holder (generally, for the push rod a quartz glass rod is used for operation upto 1273K and alumina rod is used above 1273K) pressed lightly against specimen. A certain amount of pressure was applied for mounting the sample to ensure proper contact. A cryostat, capable of heating in the range of 103K to 573K temperature, was used which enclosed the whole sample holder - push rod assembly. The change in length was transferred through the push rod to an inductive pick-up which works on the linear variable differential transformer (LVDT) principle. The output voltage was fed to a X-Y recorder where the change in length was directly recorded. The temperature of the specimen was measured by a chromel-alumel thermocouple and continuously recorded on the second channel of the X-Y recorder. the CTE measurement was done in the ambient to 373K temperature range at a heating rate of 1K/min. The following formula was used to calculate the CTE value,

$$\text{CTE} = \frac{1}{L_0} \cdot \frac{\Delta L}{\Delta T} \cdot \left(\frac{1}{K}\right)$$

where, L_0 = Initial length of the sample in the ambient temperature, ΔL = Change in length and ΔT = Testing temperature range.

Chapter 5

RESULTS AND DISCUSSION

5.1 Characterization of MA Invar Powder

5.1.1 X-Ray Diffraction Studies

The X-ray diffraction patterns of Invar powder mechanically alloyed for different time durations such as 2 hours, 4 hours, 8 hours, 16 hours, 24 hours and 32 hours are illustrated in Fig.5.1 along with the diffraction pattern of the starting 64Fe-36Ni powder aggregate (0 hour). Fig.5.1 shows progressive mechanical alloying of Ni with Fe with time at room temperature.

The Fe-Ni binary alloy system has complete liquid miscibility and Ni has appreciable solid solubility in Fe at room temperature (see the Fe-Ni binary phase diagram in Fig.2.2). These facts made the room tempareture mechanical alloying of Ni with Fe less difficult. Fe, Ni and Fe-Ni alloy of 64Fe-36Ni composition, all have their strongest characteristic X-ray peaks in the 43.5^0 to 45^0 in 2θ values, which overlap each other. For this Fe(200) peak occurring at 65.02^0 an Ni(220) peak occurring at 76.37^0 in 2θ are chosen as the reference peaks for the determination of mechanical alloying. It can be established from Fig.5.1 that the relative intensity of these two peaks diminished with progress in milling which indicates the alloying of Ni with Fe to form Fe-Ni alloy. At around 32 hours of milling these two reference peaks almost became non-existent while the strongest peaks of Fe(110) and Ni(111) also showed substantial reduction in intensity. At this stage a small peak at 43.5^0 is observed, which after indexing with the help of ASTM Powder Diffraction File, is found to be from the (111) plane of the Fe-Ni alloy. So, the 32 hours of milling is

Table 5.1: Chemical composition of MA Invar

Constituent	Iron	Nickel	Tungsten carbide
wt%	65.61	31.56	2.83

found to be the optimal time for the preparation of MA Invar powder.

5.1.2 Size Distribution and Shape of MA Invar Powder

The particle size distribution of the Invar powder, mechanically alloyed in argon gas atmosphere for 32 hours, was obtained from the standard sieve analysis test. The particle size distribution is shown in Fig.5.2 in the form of a histogram which shows a skewness towards finer particle size. Almost 80% of the powder was found to be below 400 mesh (BS) size.

The shape of the Invar powder obtained in the present study is shown in the SEM photomicrograph in Fig.5.3. The powders are rough and irregular shaped since they are formed predominantly by cold welding and fracturing of free powder particles.

5.1.3 Chemical Composition

The bulk chemical composition of the MA Invar powder was arrived at by conducting EMPA studies on a powder compact. The bulk chemical composition, an average of 20 test points, is given in Table-5.1 (see Appendix-1 for the procedure of calculation),

The starting material was 64%Fe-36%Ni powder aggregate but this composition could not be achieved in the final MA Invar powder because of relatively greater loss of Ni powder than Fe powder through the shaft clearence in the attritor mill during milling operation. The reason for this differential loss could possibly be attributed to the finer particle size of the starting Ni powder, which had almost 85% of its powder mass below 400 mesh size while the starting Fe powder had 50% of its powder mass below 400 mesh size (see section 4.1 in Chapter-4).

Though tungsten is appearing in the bulk composition it is not present in the alloy in solid solution, instead it is present as tungsten carbide in the finely dispersed form. The bulk carbon content (as WC) could not be analyzed because of the technical limitation of the EMPA device. But the presence of WC was confirmed by the qualitative EMPA

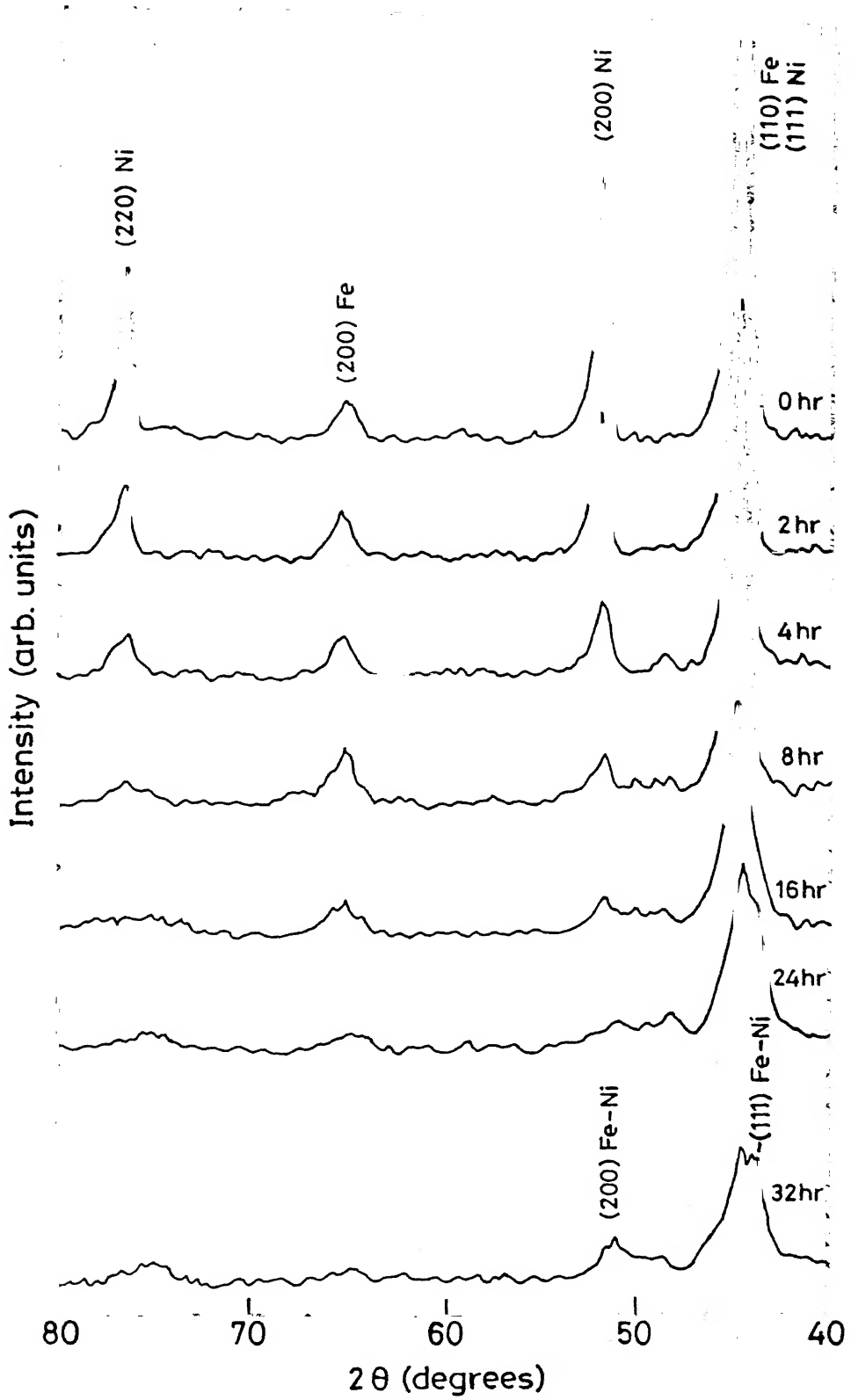

Figure 5.1: X-ray diffraction pattern of MA Invar powder showing progress of mechanical alloying with milling time (in hours)

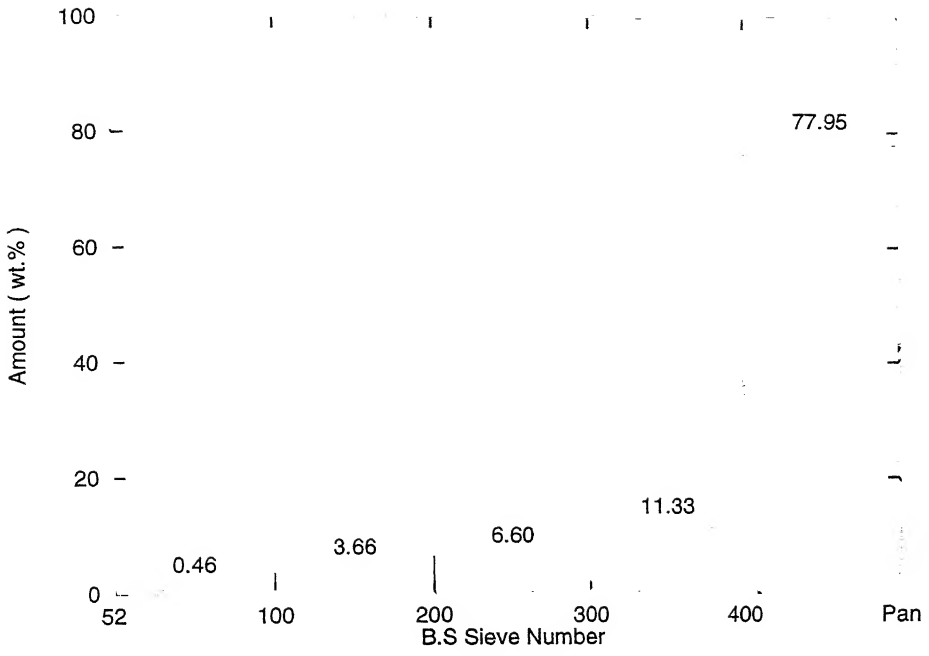

Figure 5.2: Particle size distribution of MA Invar powder

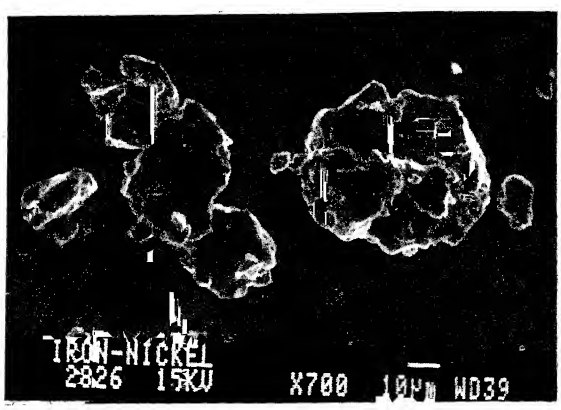

Figure 5.3: SEM photomicrograph of MA Invar powder

test carried out on the fractured Invar strips which is discussed in section 5.2.4. The fine WC particles came from the worn out WC balls, used during mechanical alloying as the grinding media.

5.2 Characterization and Properties of Monolithic Invar Strip

5.2.1 Microstructural Evolution and Hot Rolling Behaviour of The Sintered Strip

The microstructure of the sintered, full density hot rolled and post-densification annealed strips in the etched condition are shown in Fig.5.4 (a), (b) and (c) respectively.

The sintered structure shows loosely sintered aggregate of the powder particles. In the full density hot rolled structure elongated grains of the single phase alloy are observed while the post-densification annealed structure shows not much change from the hot rolled structure which is probably due to the low annealing temperature (973K being $0.56T_m$ for Invar where T_m is the melting range of Invar in absolute scale of temperature).

The full densification was achieved at ~80% hot rolling reduction which was confirmed by microscopic observation and density mesurements (discussed in the next section). The initial sintered density of ~47% of theoretical density should ideally require ~60% hot reduction to achieve full density. But it required ~80% hot reduction since some amount of rolling reduction was spent in the elongation of the strip, the rest utilised in closing the pores present in the sintered strip. Moderate amount of edge cracking was observed during hot rolling of the monolithic Invar strip.

5.2.2 Density

The sintered density of the Invar strip was found to be ~47% of the theoretical density and the average density of the ~80% hot rolled Invar was found to be 8.287 g/cc. which is 99.96% of the theoretical density. Theoretical density of Invar alloy of the composition obtained in the present study, is calculated by taking into cosideration the individual contribution of the different constituents of the alloy powder (see Appendix-2).

(a)

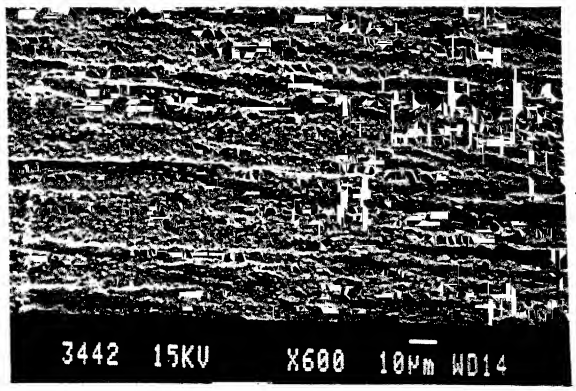

$RD \Rightarrow$

(b)

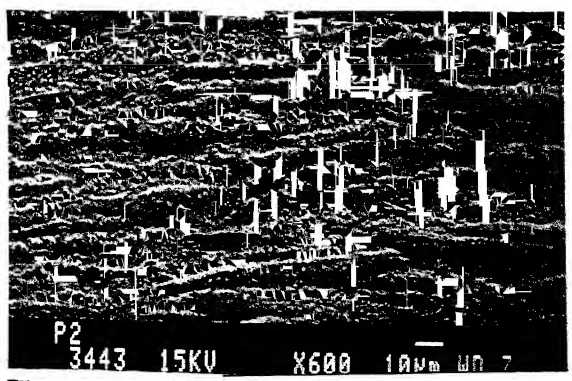

(c)

Figure 5.4: SEM photomicrograph showing microstructure of (a) sintered, (b) full density hot rolled (c) post-densification annealed monolithic Invar strip

Table 5.2: Mechanical properties of Invar strip

Properties	Values
0.2% Proof Strength	428 MPa
U.T.S	590 MPa
% Elongation	18

5.2.3 Mechanical Properties

The room temperature mechanical properties of the post-densification annealed Invar, found out by the tension test, are as shown in Table 5.2,

A typical load-elongation curve for monolithic Invar is shown in Fig.5.5 which shows continuous yielding phenomenon which is characteristic of a ductile alloy.

The mechanical strength properties of annealed Invar produced through the conventional route is discussed by Duffaut and Cozar [31]. The reported values of 0.2% Proof strengh, U.T.S and % Elongation are 300 MPa, 500 MPa and 30 respectively. In the present study the observed strength values are on the higher side and elongation value is on the lower side for the PM Invar. There could be two possibilities that lead to these unususal properties. One could be the presence of finely dispersed WC particles which imparts dispersion strengthening to the overall matrix. The other possibility is the presence of some amount of cold work in the annealed strip even after annealing at 973K for 1800s. The first possibility is confirmed by the results of the EMPA studies carried out on the fractured surface of the tension test specimen, discussed in the next section. The second possibility needs further investigation.

5.2.4 Fractography

The SEM photomicrographs of fractured surface of the monolithic Invar specimen after tension test are shown in Fig.5.6 (a) and (b). Fig.5.6(a) shows a typical ductile fracture characterized by the presence of dimple structures. Fig.5.6(b) clearly shows the inclusion seated at the centre of one such typical dimple structure. The inclusion size was found to be $0.3\mu m$ in diameter. The nature of the inclusion was detected to be tungsten carbide (WC) by carrying out EMPA studies on that particular inclusion site. The corresponding qualitative EMPA result is shown in Fig.5.7 which shows characteristic X-ray signals

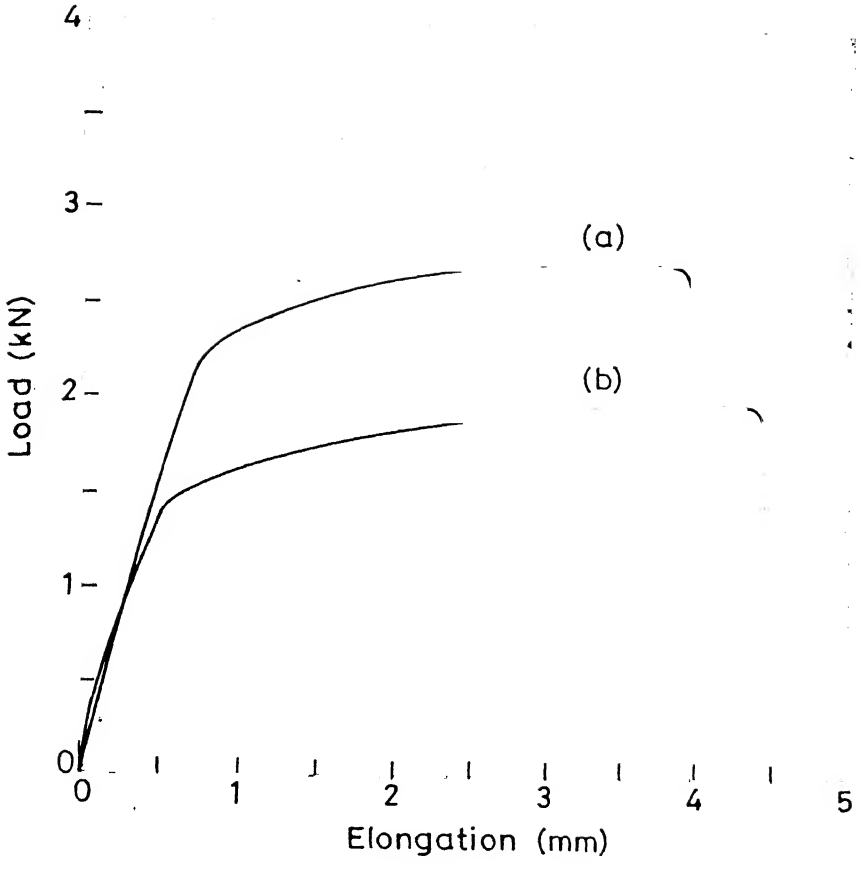

Figure 5.5: Typical load-elongation curve obtained for (a) monolithic Invar and (b) Copper-Invar-Copper laminated strips

of tungsten and carbon obtained from that particular inclusion along with the strong background iron and nickel signals.

5.2.5 Coefficient of Thermal Expansion (CTE)

The average CTE of hot rolled and subsequently annealed monolithic Invar was found to be 5.76 $\times 10^{-6}$/K in the 293K to 373K temperature range. The sample taken from the tension tested specimen showed an average CTE of 5.70 $\times 10^{-6}$/K.

The average CTE values are well in agreement with the values reported for the alloy of this particular composition produced through the conventional route. From the works of Guillaume [37] it is found that the CTE value for an Invar alloy with a $\sim$ 32% Ni content falls in the range of 5 – 6 $\times 10^{-6}$/K. Fig.2.3 shows the behaviour of CTE with composition of Fe-Ni alloys. The values obtained in the present study can be improved upon if the WC contamination in the alloy powder is checked by taking some suitable precautions during alloy powder production.

5.3 Characterization and Properties of The Copper-Invar-Copper Laminated Strips

5.3.1 Density

The average relative density of the individual sintered layers of the Cu-Invar-Cu laminated strip was found to be 0.47 for the Invar core and 0.44 for the Cu layers. The average density of the fully densified (85% hot rolled) Cu-Invar-Cu laminatd strip was found to be in the range of 8.49 - 8.51 g/cc which is 99.88% to 100.1% of the theoretical density calculated by applying the rule of mixture taking average Cu : Invar : Cu thickness ratio to be 15.5 : 69 : 15.5 in the fully densified strip (see Appendix-3). There is difficulty in determining the actual densification occurred in the laminated strip by density measurement, since percentage densification is calculated on the basis of the theoretical density value which is error prone as it is determined on the basis of the Cu : Invar : Cu ratio in the final strip measured by metllographic technique. Nevertheless, the 85% hot rolled strip can be considered as fully densified.

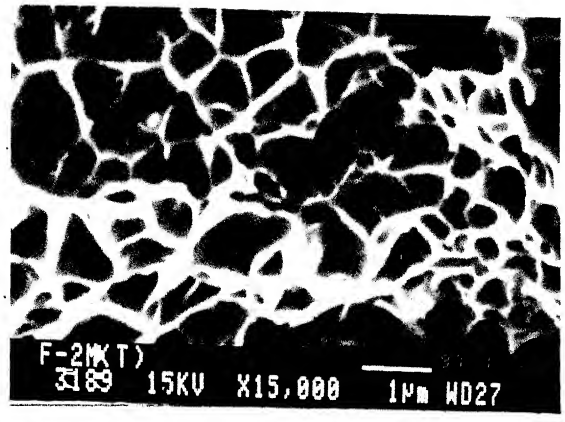

(a)

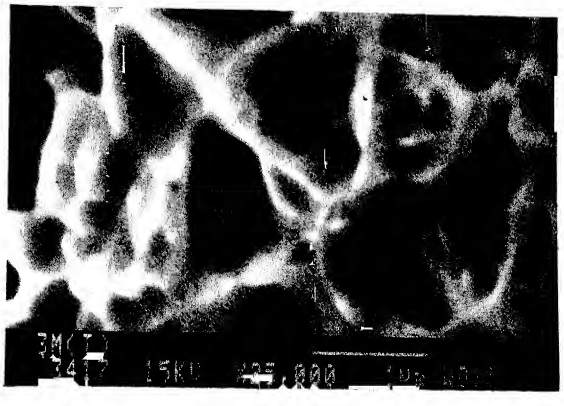

(b)

Figure 5.6: SEM photomicrograph of the fractured surface of the monolithic Invar strip showing (a) dimple structure and (b) inclusion particles seated at the centre of one such dimple structure.

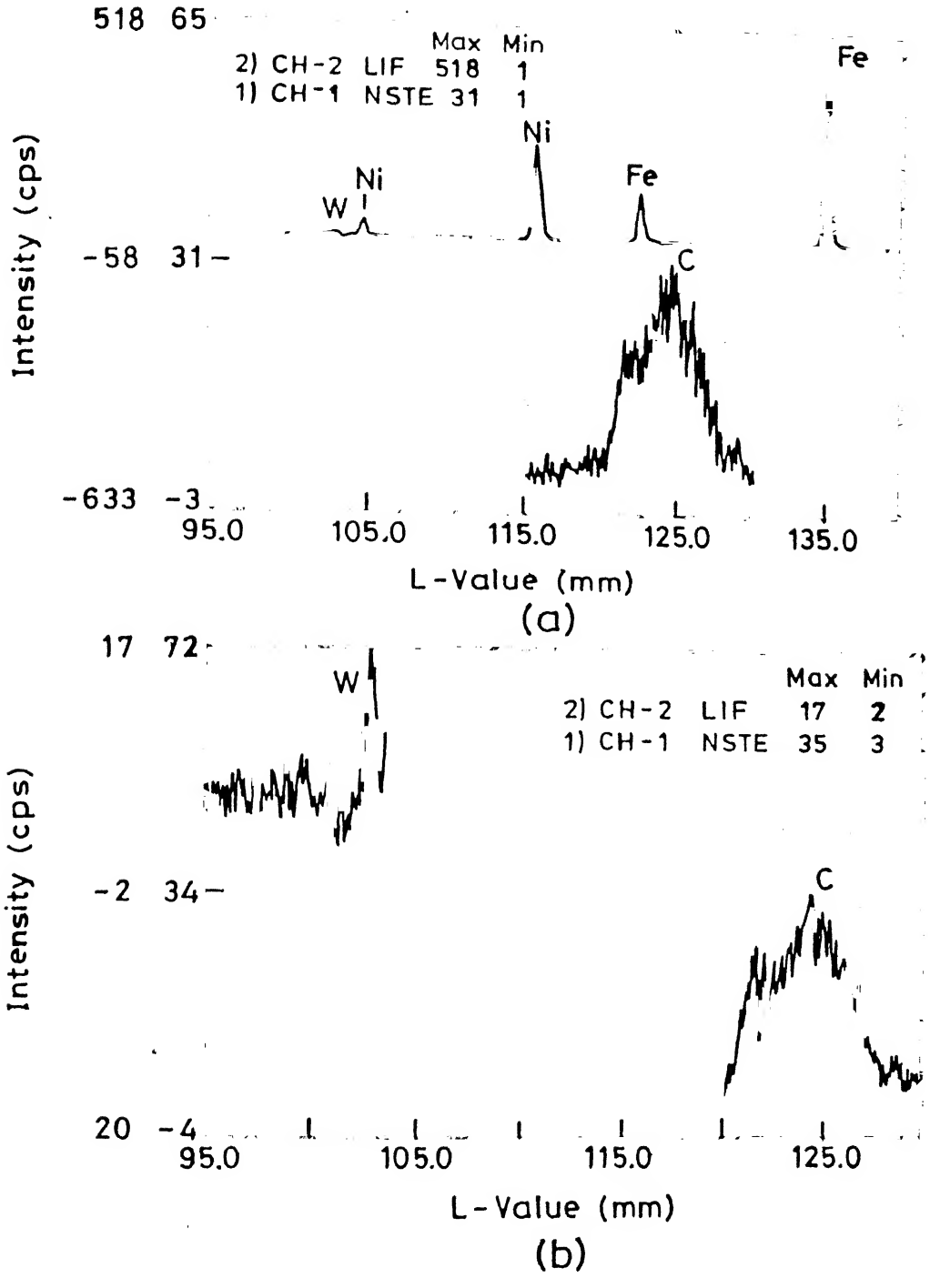

Figure 5.7: Spectral lines of different elements at the inclusion site obtained from the qualitative EMPA studies showing (a) all the constituent elements and (b) only tungsten and carbon.

5.3.2 Microstructural Evolution

The SEM photomicrographs of Copper-Invar interface at sintered, different degrees of hot rolled, full density hot rolled and post-densification annealed conditions in the etched state are shown in Fig.5.8 to 5.11. Fig.5.8 shows the sintered structure while 24%, 32%, 53% and 66% single pass hot rolled structures are shown in Fig.5.9 (a), (b), (c) and (d) respectively. The multi-pass hot rolled structures of 72%, 77%, 83% and 85% cumulative hot reduction are shown in Fig.5.10 (a), (b), (c) and (d) respectively. Fig.5.11 shows the post-densification annealed microstructure.

The densification in monolithic porous metal strips during hot rolling occurs through the following mechanisms,

1. Transitional restacking of particles.

2. Growth of contact area.

3. Longitudinal flow of particles in the rolling direction.

The initial sintered strip consisted of basically an aggregate of loosely sintered metal particles. The overall stresses acting on the strip during initial stages of deformation are, compressive in the thickness direction and tensile in the rolling direction. At the initial stages of deformation the powder particles rearrange and restack as the rolling progresses and the longitudinal elongaton in this stage is negligibly small. The end of this stage is marked by a situation when no further densification without longitudinal flow is possible by hot rolling. This situation corresponds to the closest packing among the powder particles and the relative density at which this occurs is a function of the initial size range of the metal powder. Some researchers [38, 39] have reported that this stage which is known as the stage-I of densification continues until a relative density of 0.70 has been achieved in the hot rolled strip for a particular size range powder. Densification from the relative density of 0.70 to 0.95 i.e, stage-II densification is associated with the continuous growth in interparticle contact area and increase in longitudinal elongation as hot rolling progresses. In this stage, the interconnected porosity changes to the isolated one. Densification beyond the relative density of 0.95 i.e, stage-III densification takes place through pore fragmentation and collapsing of the opposite pore surfaces until complete annihilation of porosity.

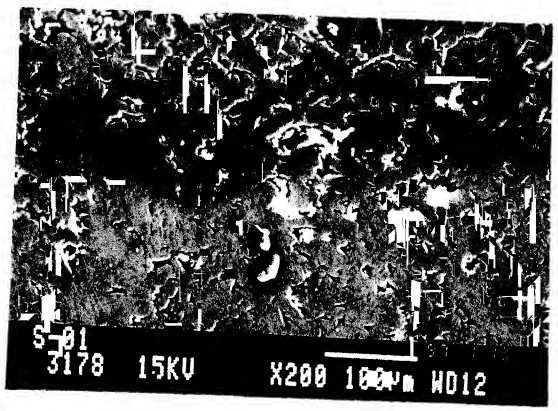

Figure 5.8: SEM photomicrograph showing microstructure of the sintered Copper-Invar interface.

In the case of trimetallic Cu-Invar-Cu strip all these three stages are visible. Fig.5.8 and 5.9(a) show stage-I, Fig.5.9(b), (c) and (d) show stage-II and Fig.5.10(a) to 5.10(d) show stage-III densification. It is observed from these figures that both copper and Invar started elongating at the early stage of hot reduction. Copper, being more ductile, elongated more than the Invar pairticles, as also found out by Katrus and Vinogradov [11]. Beyond 72% reduction (Fig.5.10(a) to 5.10(d)) both the layers elongated uniformly. At the final stages of hot rolling the volume change in the compact became negligible due to drastic reduction in the amount of porosity.

5.3.3 Microhardness Profiles

The microhardness values measured across the Copper-Invar interface at different degrees of rolling reduction are plotted with distance to form the microhardness line profiles which are shown in Fig.5.12 to 5.19. The effect of percent hot rolling reduction on the average microhardness of the copper and Invar layers are shown in Fig.5.20.

Since the microhardness values are often associated with instrumental as well as human error because of its very high sensitivity towards minimal fluctuation in the measuring conditions, these microhardness line profiles basically provide semiquantitative information. So these are not to be treated as absolute values. In all the microhardness profiles

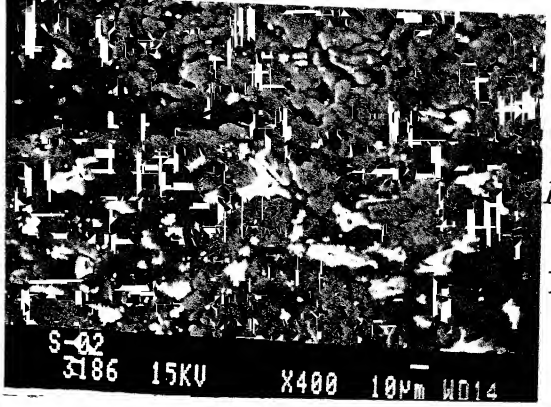

(a)

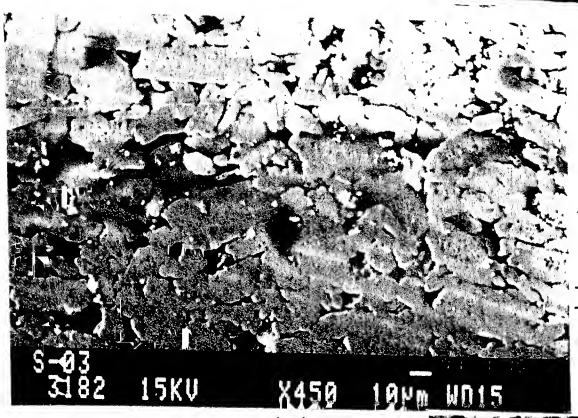

(b)

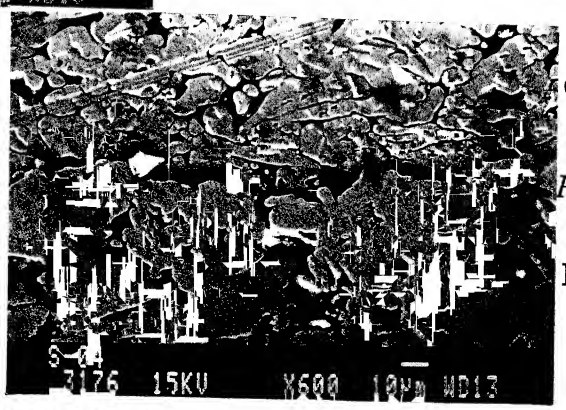

(c)

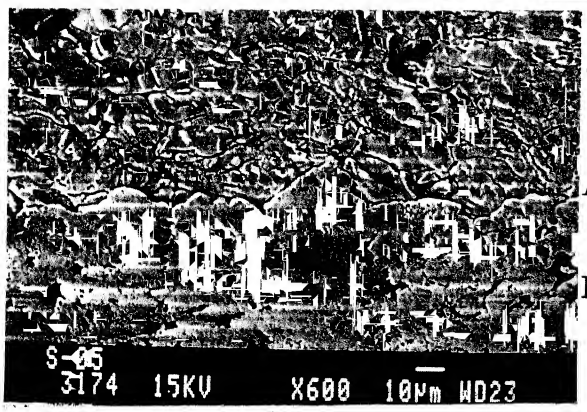

(d)

Figure 5.9: SEM photomicrograph showing different stages of densification at the Copper-Invar interface in single pass hot rolling of (a) 24%, (b) 32%, (c) 53% and (d) 66% thickness reductions.

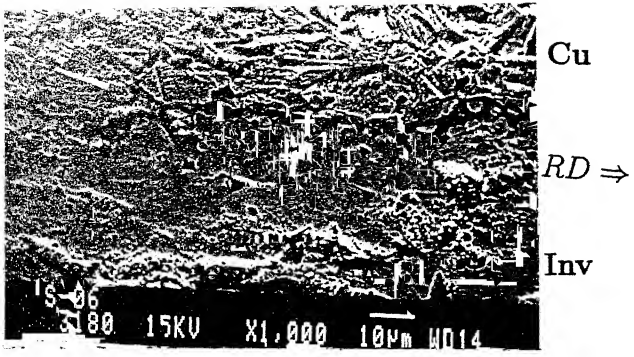

(a)

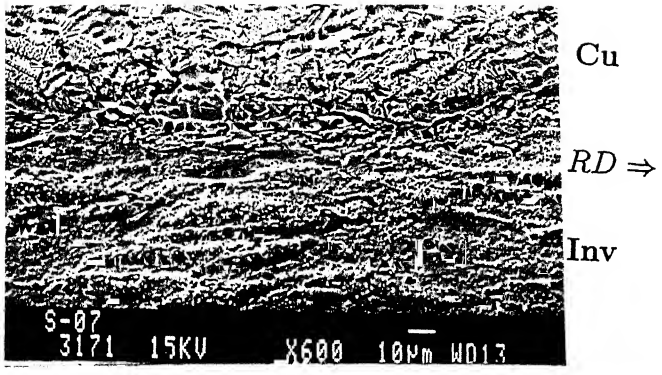

(b)

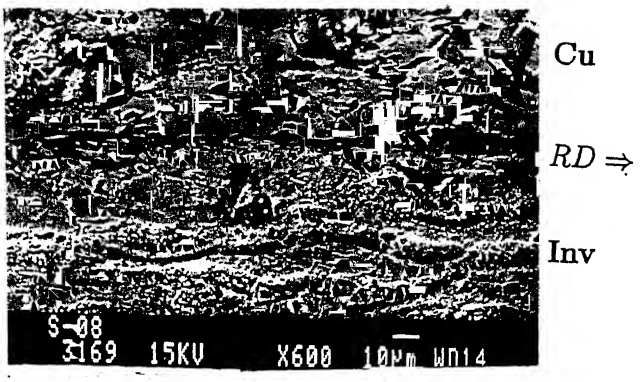

(c)

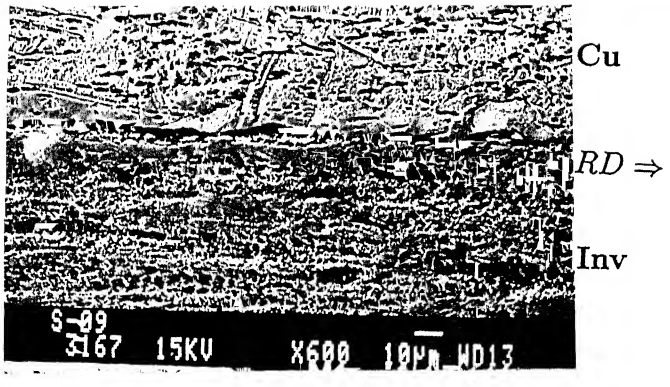

(d)

Figure 5.10: SEM photomicrograph showing different stages of densification at the Copper-Invar interface in multiple pass hot rolling of (a) 72%, (b) 77%, (c) 83% and (d) 85% thickness reductions.

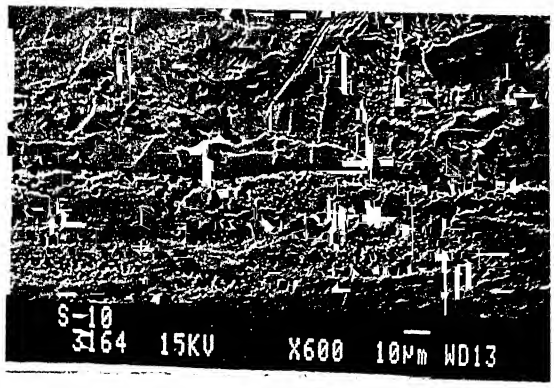

Figure 5.11: SEM photomicrograph showing microstructure of the post-densification annealed Copper-Invar interface.

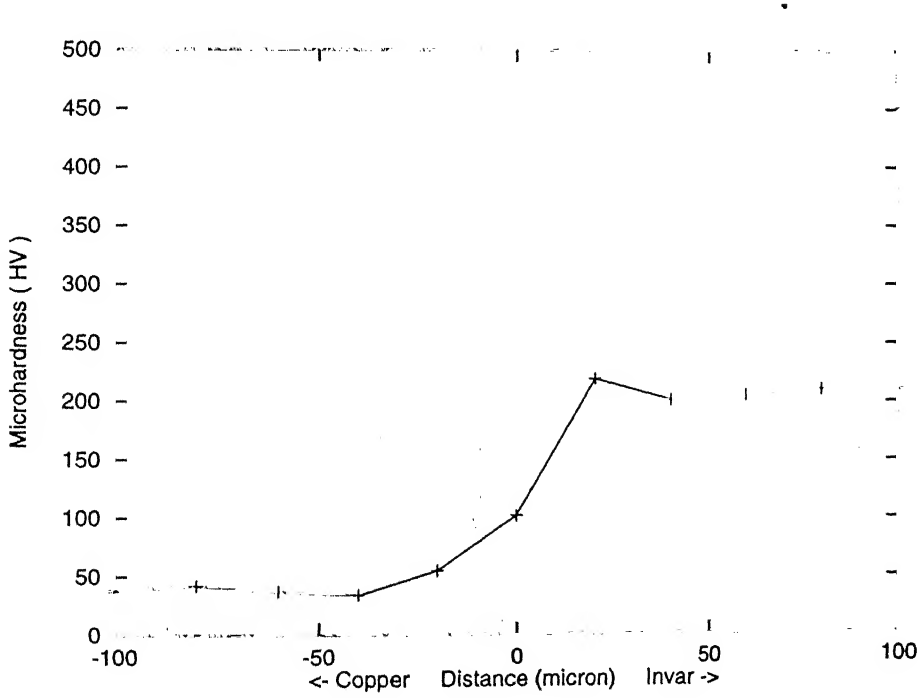

Figure 5.12: Microhardness profile of 24% hot rolled (single pass) strip

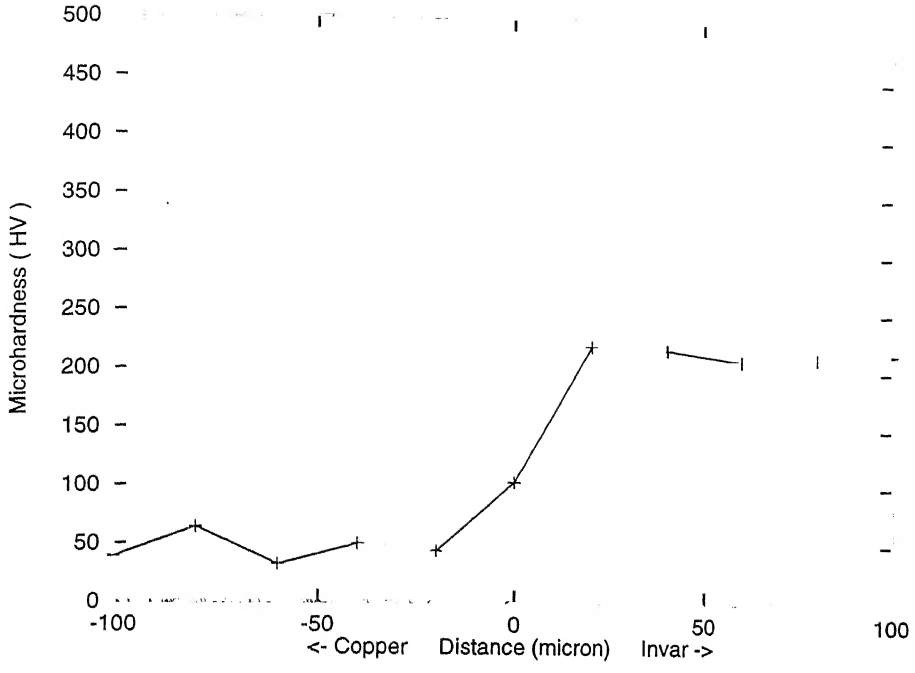

Figure 5.13: Microhardness profile of 32% hot rolled (single pass) strip

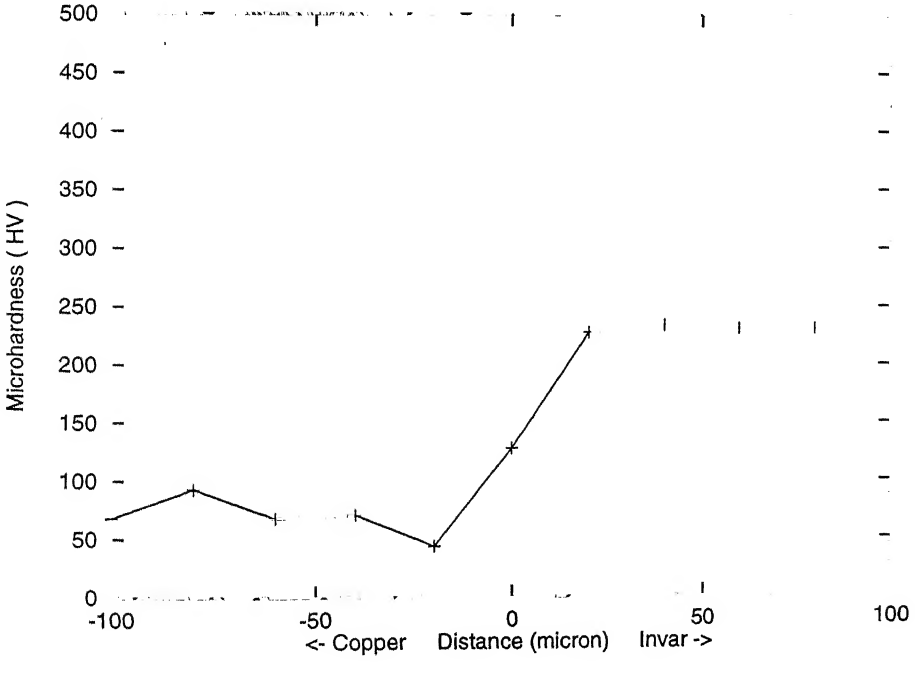

Figure 5.14: Microhardness profile of 53% hot rolled (single pass) strip

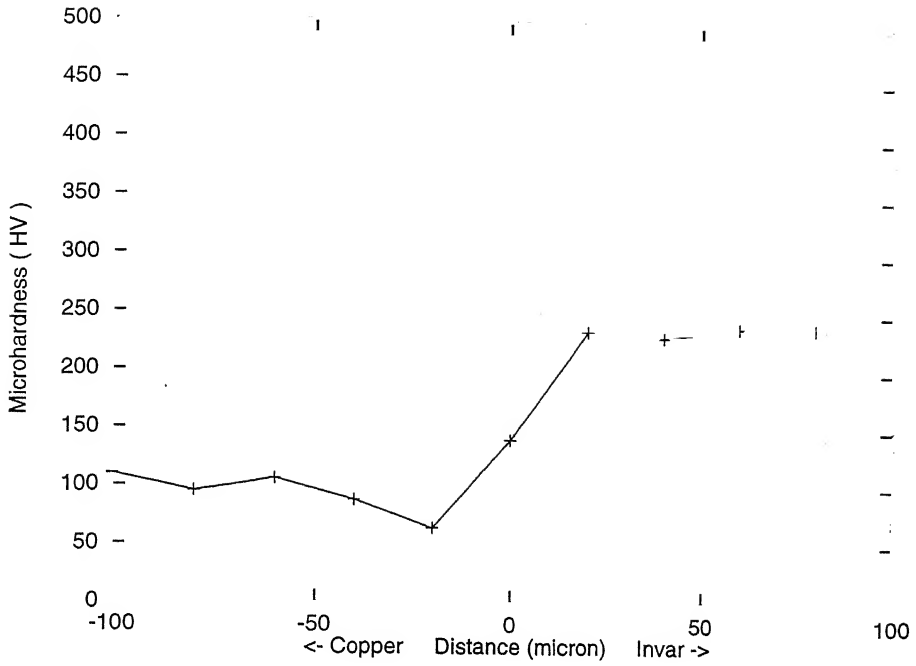

Figure 5.15: Microhardness profile of 66% hot rolled (single pass) strip

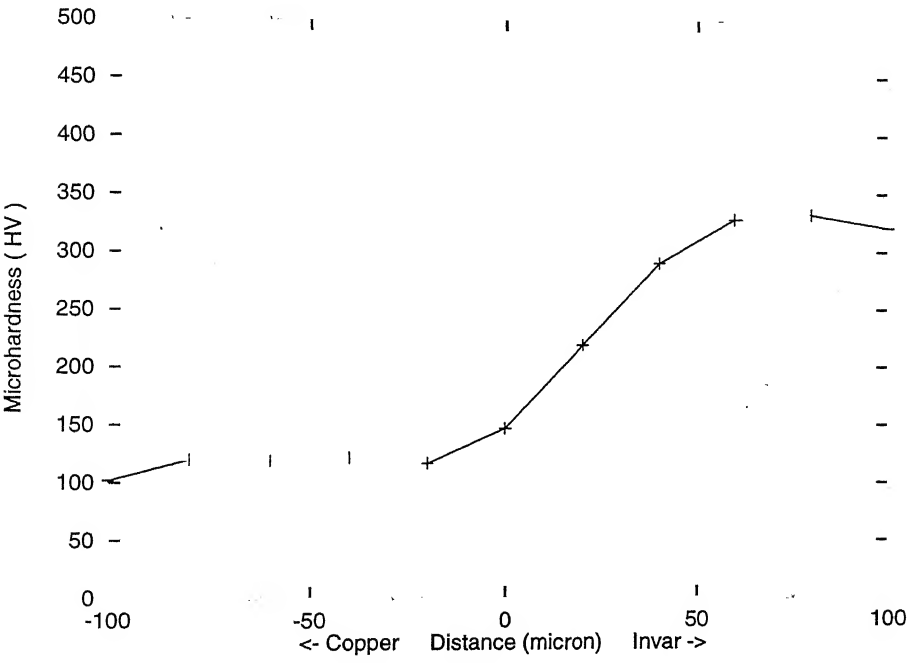

Figure 5.16: Microhardness profile of 72% hot rolled (multipass) strip

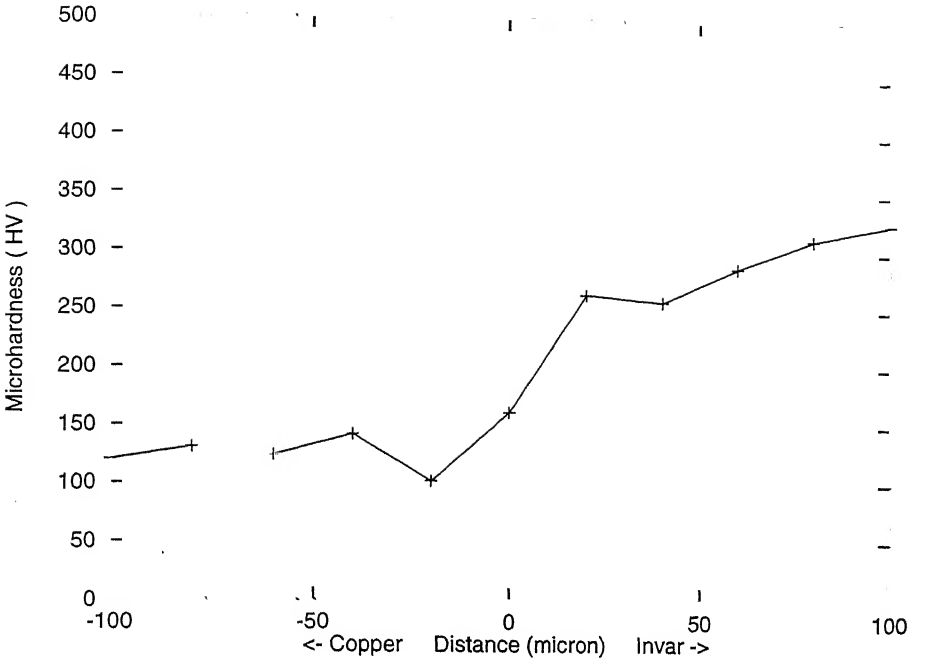

Figure 5.17: Microhardness profile of 77% hot rolled (multipass) strip

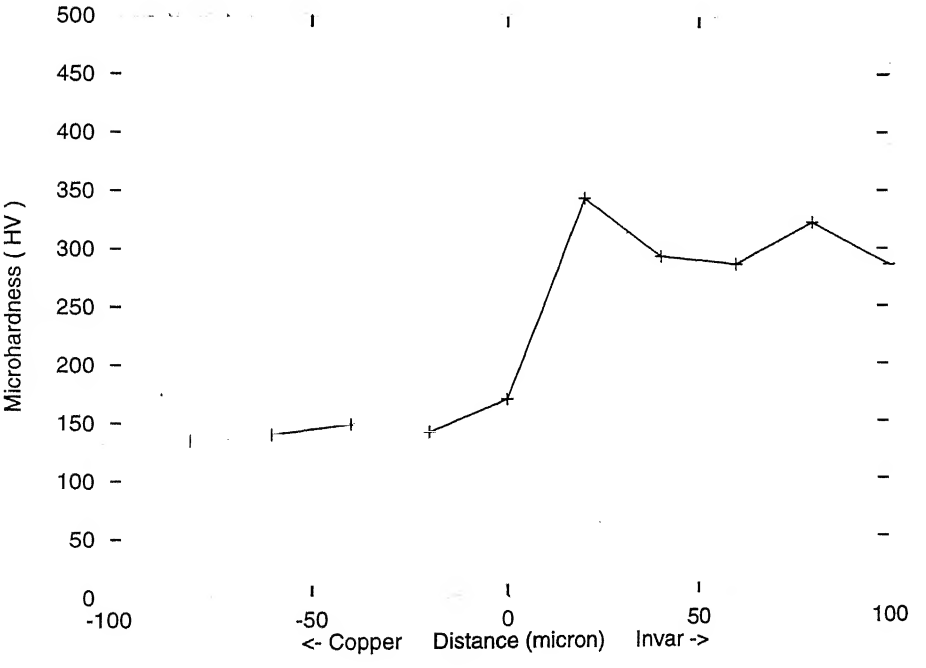

Figure 5.18: Microhardness profile of 83% hot rolled (multipass) strip

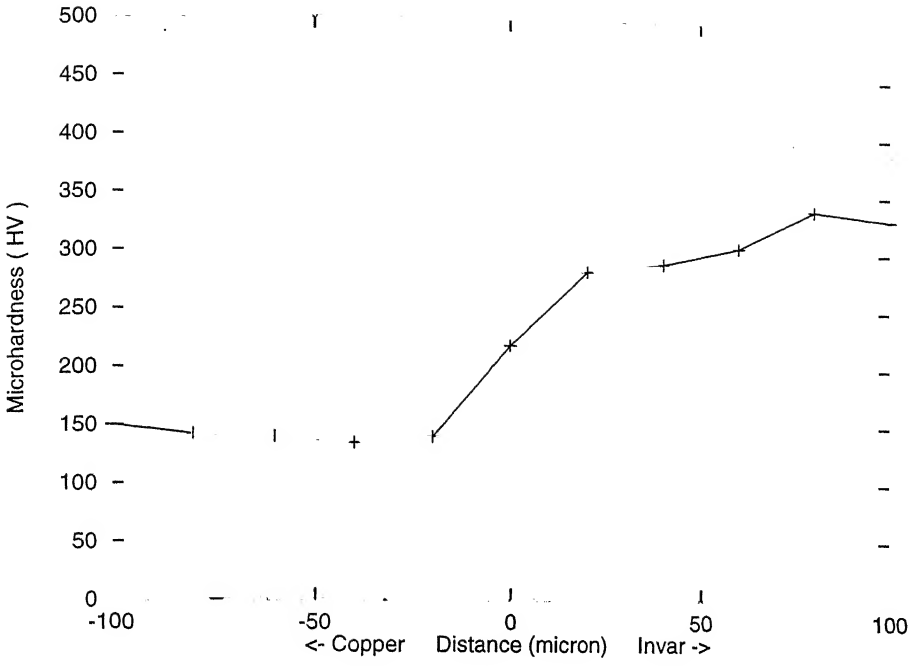

Figure 5.19: Microhardness profile of 85% hot rolled (multipass) strip

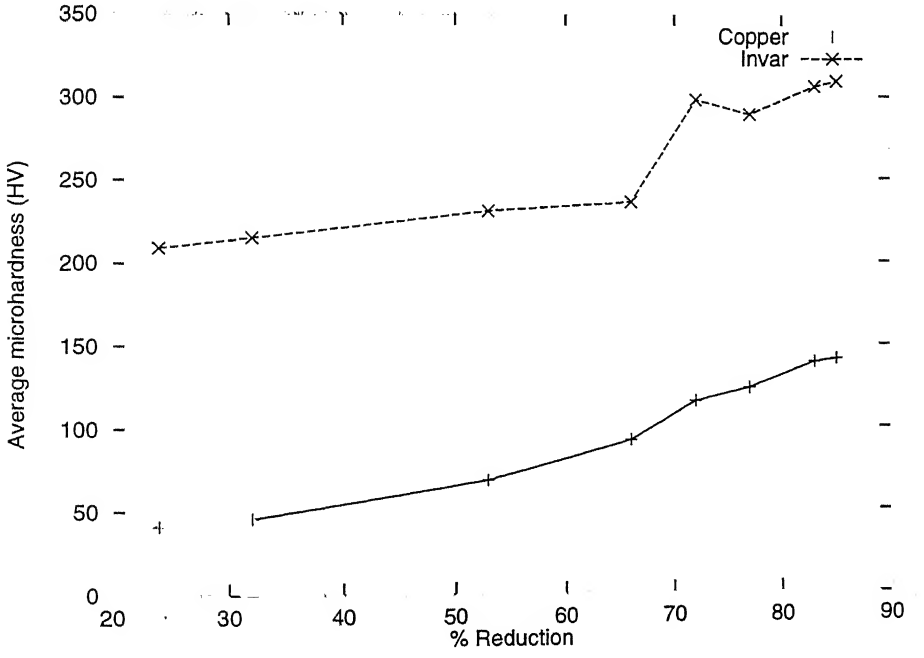

Figure 5.20: Effect of hot rolling reduction on the average microhardness profile of Copper and Invar layers.

a plateauing off of the microhardness values on either side of the interface is observed at a distance starting from $25\mu m$ off the interface. The average microhardness from the hardness plateaus on either side of the interface for different amount of hot reduction are plotted in Fig.5.20. This shows that both the copper and Invar layers got densified almost simultaneously at the higher amounts of hot rolling reductions which is confirmed by the parallelity of the two curves for copper and Invar. At the initial reductions the average microhardness increased because of increase in the degree of random dense packing, while at the higher amount of hot reduction the microhardness values increased due to reduction in porosity and overall densification. At the final stages of hot reduction the microhardness values became constant as the densification also reached a constant level.

5.3.4 Concentration Profiles

The EMPA studies were carried out across the Copper-Invar interface in the sintered, different degrees of hot rolled, full density hot rolled and post-densification annealed strips. It yielded concentration line profiles, which are shown in Fig.5.21 to 5.30. In each of the concentration profiles an average composition of 50% copper and 50% Invar (i.e, 33.2% Fe and 16.8% Ni) is chosen just at the interface point since most of the test data at the interface conformed well with this proposition. Furthermore, accurate measurement of the interface composition is quite difficult, if not erroneous, considering the sharp appearence of the interface and the technical limitations of the EMPA device.

It is observed from the concentration profiles that with increasing amount of hot rolling reduction the diffusion zone on either side of the interface is shrinking. This is more pronounced in case of diffusion of Cu in Invar layer than in the case of diffusion of Fe and Ni in the copper layer. It is further noticed that in the single pass hot reduction the shrinkage in the diffusion zone is negligible in the low reductions e.g, 24% and 32% (see Fig.5.21 and 5.22) thickness reductions which is comparable with the sintered condition, while for the higher amount of single pass reductions e.g, 53% and 66% reduction the diffusion zone shrinkage is more, see Fig.5.23 and 5.24. In case of multi-pass hot reduction a 72%, 77%, 83% and 85% cumulative hot rolling schedule was followed coupled with reheating to 973K temperature before each pass. In this case the diffusion zone further shrinks, which becomes almost 20 μm on either side of the interface at full densification (85% hot rolled condition). The post-densification annealing increases the depth of the

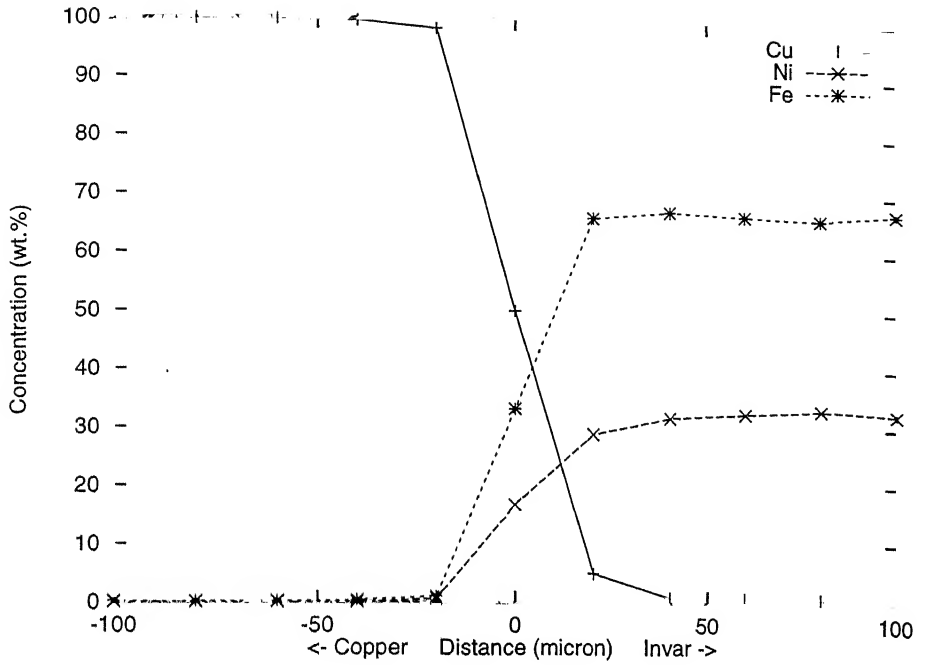

Figure 5.21: Concentration profile in sintered strip

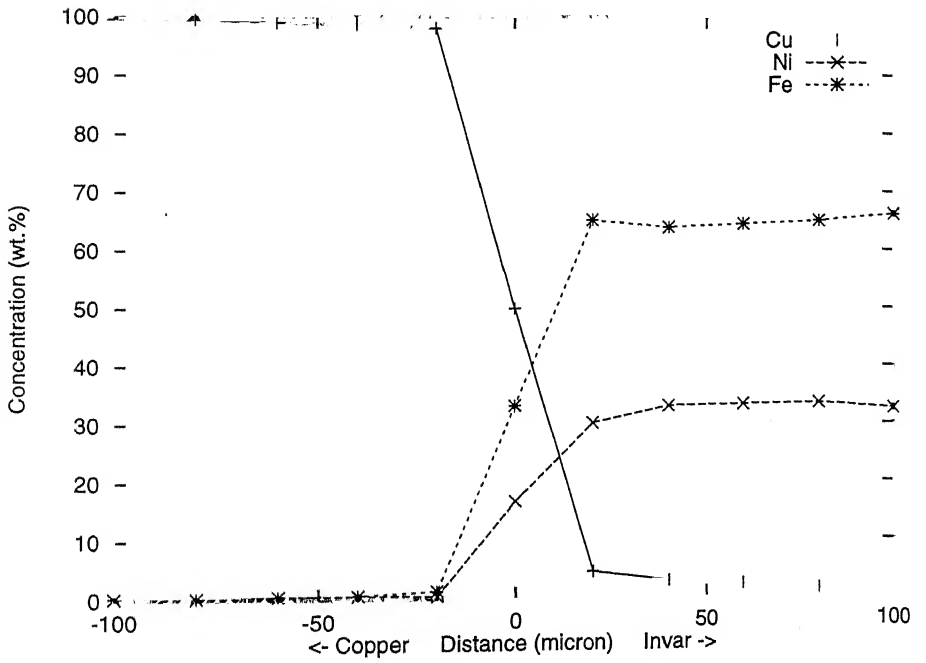

Figure 5.22: Concentration profile in 24% hot rolled (single pass) strip

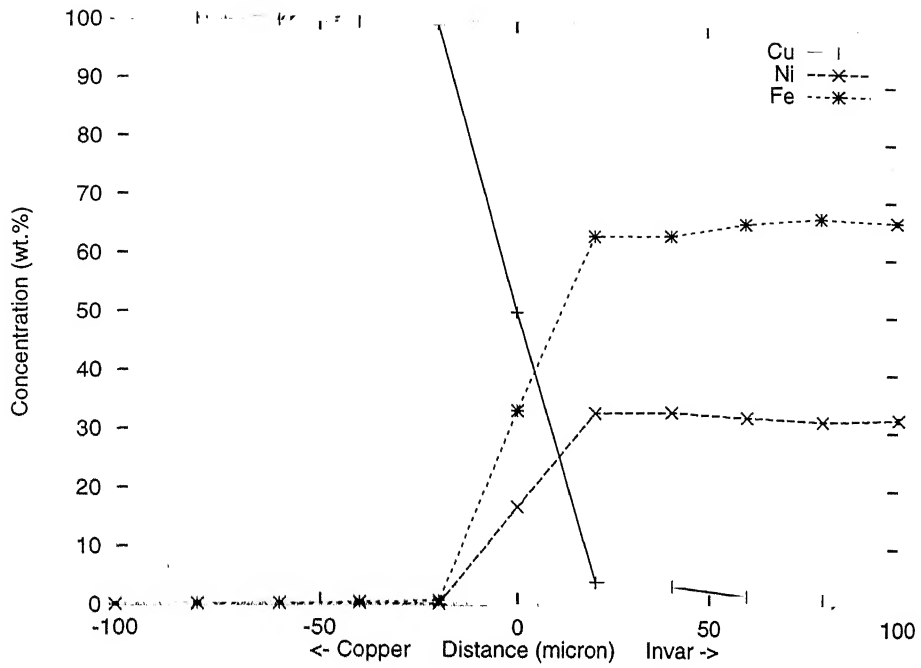

Figure 5.23: Concentration profile in 32% hot rolled (single pass) strip

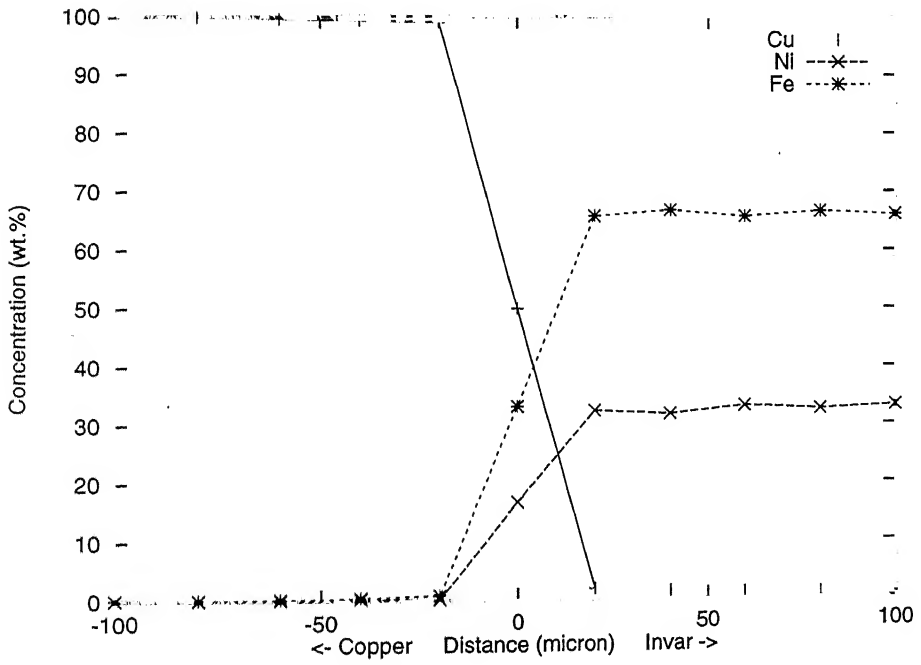

Figure 5.24: Concentration profile in 53% hot rolled (single pass) strip

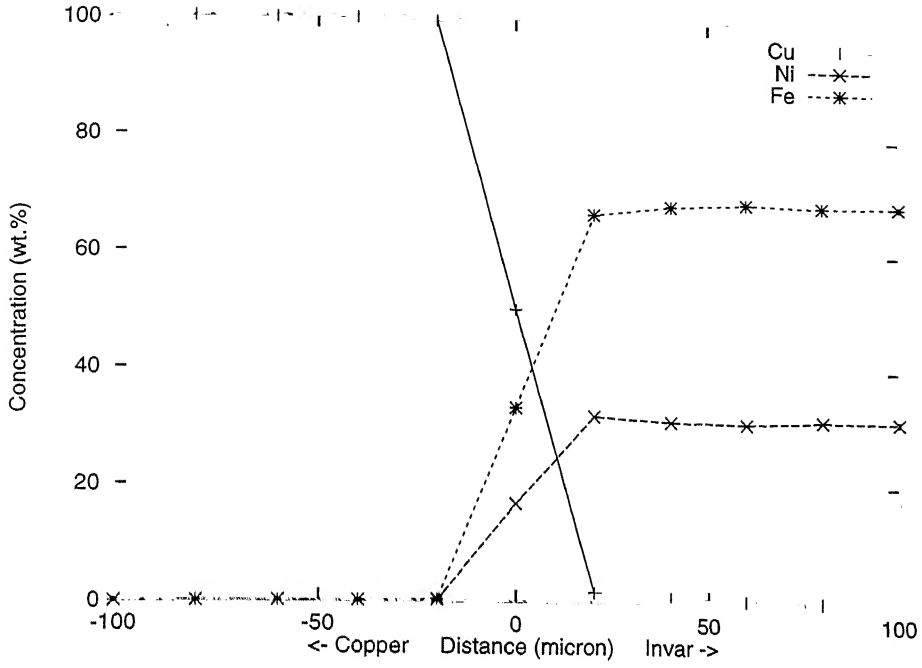

Figure 5.25: Concentration profile in 66% hot rolled (single pass) strip

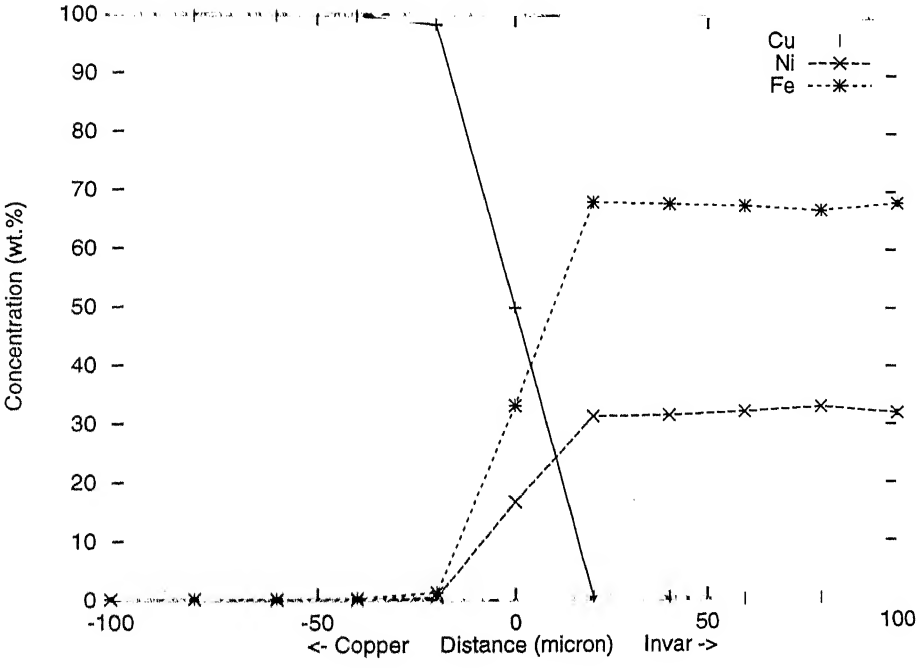

Figure 5.26: Concentration profile in 72% hot rolled (multipass) strip

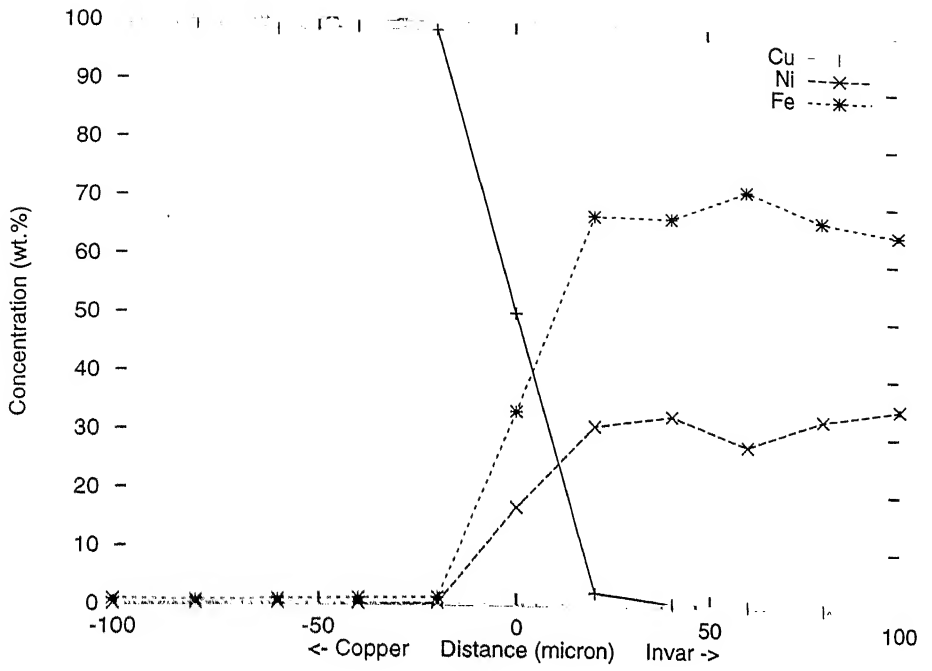

Figure 5.27: Concentration profile in 77% hot rolled (multipass) strip

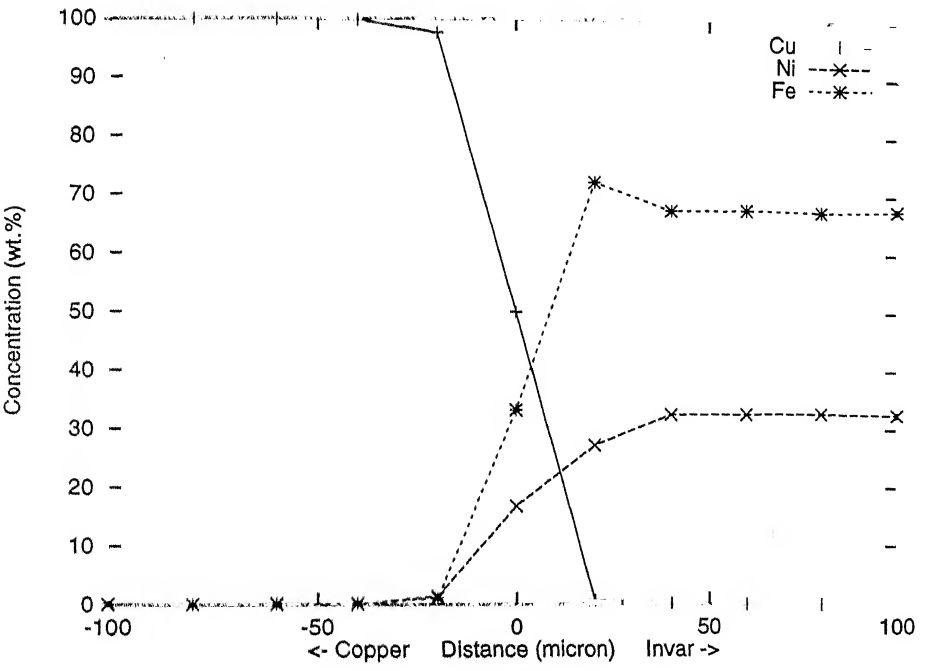

Figure 5.28: Concentration profile in 83% hot rolled (multipass) strip

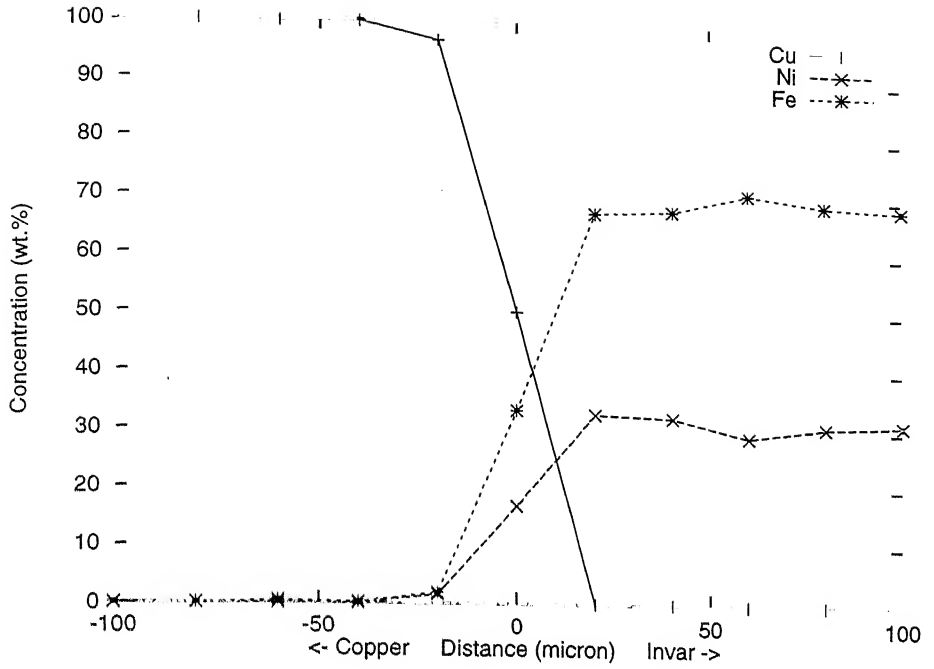

Figure 5.29: Concentration profile in 85% hot rolled (multipass) strip

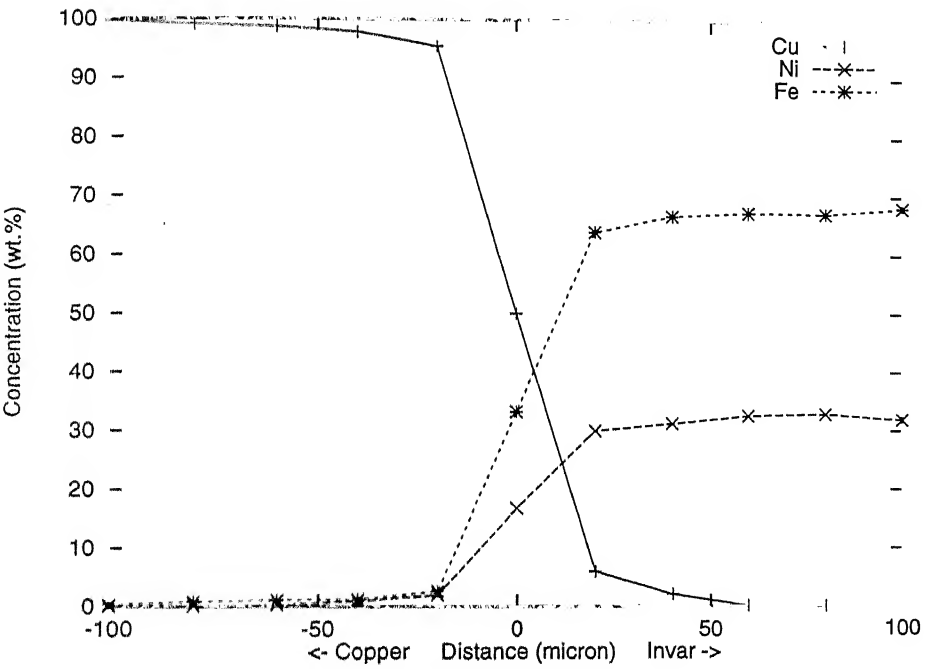

Figure 5.30: Concentration profile in post-densification annealed strip

diffusion zone to 50 μm on either side of the interface.

Since at the initial stage densification takes place by restacking and rearrangement among the powder particles and the degree of densification is low at this stage, the diffusion zone shrinkage is negligibly small e.g, in the case of 24% and 32% single pass hot reductions. With further densification as for example 53% and 66% single pass hot reductions, the relative density of both the layers increased along with some amount of longitudinal elongation. Thus the original diffusion zone formed during sintering gets compacted and somewhat elongated resulting in the depthwise shrinkage in the diffusion zone on either side of the interface. In the multipass hot rolling schedule, eventhough the strips experience more reheating cycles (with cumulative hot reduction) than the single pass hot rolled strips, they eventually show smaller depth of diffusion zone since longitudinal elongation is more pronounced at these higher amount of hot reductions. This causes the diffusion zone to elongate perpendicular to the thickness direction. Simultaneously the diffusion zone should also increase in the thickness direction because of exposure to more reheating cycles. But the longitudinal elongation more than compensates for the increase in the diffusion zone due to reheating. This is reflected in the smaller depth of diffusion zone of the order of $20\mu m$ on either side of the interface in the fully densified (85% hot rolled) condition. Though the post-densification annealing increased the depth of the diffusion zone to $50\mu m$, it is still quite small compared to the overall strip thickness of $1000\mu m$ ($=$ 1mm) thereby having very small influence on the physical properties of the individual layers.

From the study it is clear that with rolls of suitable dia. if the full densification is achieved through a single pass rather than a multi-pass schedule, the diffusion zone can be restricted to a very small depth as the reheating cycles, which increases the depth of the diffusion zone, can then be done away with.

5.3.5 Mechanical Properties

The room temperature mechanical properties of the post-densification annealed Copper-Invar-Copper laminated strip found out by the tension test are shown in Table 5.3,

A typical load-elongation curve is shown in Fig.5.5 along with the same curve for the monolithic Invar for direct comparison purpose. The average Cu : Invar : Cu thickness ratio in the final strip is found out to be 15.5 : 69 : 15.5. Now applying the mixture rule

Table 5.3: Mechanical properties of Cu-Invar-Cu laminated strip

Properties	Values
0.2% Proof Strength	325 MPa
U.T.S	486 MPa
% Elongation	21

for the theoretical strength properties in the final strip, the 0.2% Proof Stregth and the U.T.S are calculated to be 324 MPa and 480 MPa respectively (see Appendix-4). The experimentally obtained strength values exactly match with the theoretical values. Thus it is confirmed that the rule of mixture which is generally used in calculating the properties of composites can also be used in the Copper-Invar system.

5.3.6 Fractography

The SEM photomicrographs of the fractured surface of the Cu-Invar-Cu laminated strip specimen after tension test are shown in Fig.5.31(a) and (b). The characteristic dimple structure is seen in the Invar core while fibrous fracture is seen in the laminated copper layer (see Fig.5.31(b)), which is the characteristic feature of the failure of ductile copper under the uniaxial tensile loading.

5.3.7 Coefficient of Thermal Expansion (CTE)

The average CTE of post-densification annealed Cu-Invar-Cu laminatd strip is found to be 8.15 $\times 10^{-6}$/K in the 293K to 373K temperature range while the sample taken from the tension tested specimen showed an average CTE of 9.2 $\times 10^{-6}$/K. The higher value in the tension tested specimen could be due to the elongated grains of copper or could be due to higher amount of copper present in the specimens than that presumed since the chance of error in finding the average thickness ratio of Copper to Invar through metallographic techniques is always appreciably high. This phenomenon needs further investigation.

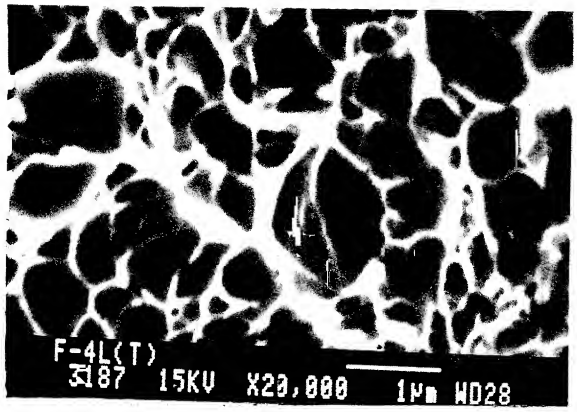

(a)

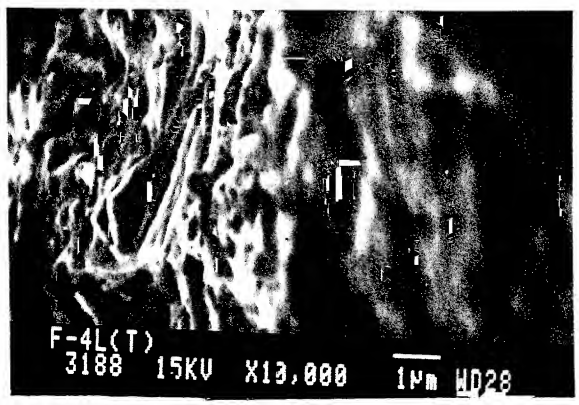

(b)

Figure 5.31: SEM photomicrograph of the fractured surface of the Copper-Invar-Copper laminated strip showing (a) dimple structure in the Invar core and (b) fibrous ductile fracture of the Copper laminated layer.

Chapter 6

CONCLUSIONS

The following conclusions can be drawn from the present study,

1) Monolithic Invar strip of $\sim$ 1mm thickness was successfully prepared from mechanically alloyed Invar powder through the Powder Metallurgy slurry route comprising of slurry casting $\rightarrow$ sintering $\rightarrow$ hot densification rolling. The Copper-Invar-Copper laminated strip of $\sim$ 1mm thickness having average Cu : Invar : Cu thickness ratio of 15.5 : 69 : 15.5 was successfully prepared following the same PM slurry route with a modified three stage casting followed by sintering and hot densification rolling. This process route is suitable potential for continuous processing which requires extensive further study.

2) The fully densified and subsequently annealed (at 973K for 1800s) monolithic Invar strip prepared from MA Invar powder showed a tensile strength of 590 MPa and 0.2% proof strength of 424 MPa with a tensile elongation to failure of $\sim$ 18%. The strength values are $\sim$ 20% in excess to and elongation value is $\sim$ 40% lower than the corresponding values of the conventional annealed Invar strip. However, the percent elongation value is sufficient enough for many applications. This difference in mechanical properties is due to the presence of some amount of cold work and fine dispersion of tungsten carbide particles of submicron size in the structure which came from the worn out tungsten carbide balls used during the mechanical alloying process of Invar powder preparation.

The fully densified and then annealed (at 973K for 1800s) Copper-Invar-Copper laminated strip showed a tensile strength of 486 MPa and 0.2% proof strength of 324 MPa with a tensile elongation to failure of $\sim$ 21%.

3) The annealed monolithic Invar showed an average CTE of 5.76 $\times 10^{-6}$/K which compared well with the CTE value (in 6 $\times 10^{-6}$/K) of the annealed

conventional Invar of the similar chemical composition (Fe $\sim$ 32%Ni). This CTE value can be further improved by reducing the tungsten carbide contamination in the alloy by adopting some suitable precautions.

The annealed Copper-Invar-Copper laminated strip having average Cu : Invar : Cu thickness ratio of 15.5 : 69 : 15.5 showed an average CTE of 8.15 $\times 10^{-6}$/K which is satisfactory considering the chemical composition of Invar used in the present study.

4) The microscopic and EMPA studies carried out on the Copper-Invar interface clearly show that a metallurgical bond between the different layers is obtained by the interdiffusion of different constituent elements.

5) The diffusion zone depth for different elements such as Cu in Invar layer, and Fe and Ni in copper layer was found to be of the order of $20\mu m$ on either side of the Copper-Invar interface in the final full density hot rolled Copper-Invar-Copper laminated strip eventhough the hot densification rolling was carried out in more than one pass. With appropriately designed rolling mills it would be possible to hot roll the sintered Copper-Invar-Copper laminated strip in a single pass to full density level, which would further reduce the depth of the diffusion zone. The smaller size of the diffusion zone is beneficial for the individual physical properties of both the layers which could be impaired if large scale interdiffusion is permitted.

Chapter 7

SUGGESTIONS FOR FUTURE WORK

1) In the present study the mechanically alloyed Invar powder got contaminated by the tungsten carbide particles coming from the worn out tungsten carbide balls used as the grinding media. Therefore, a suitable alternative could be the use of Ni coated balls as the grinding media which should be systematically studied keeping in mind the control of Ni content in the final Invar powder since elemental Ni from the Ni coated balls can increase the Ni content of the final Invar powder.

2) The microscopic study of the Copper-Invar interface in the Copper-Invar-Copper laminated strips having different amounts of rolling reduction gave a very qualitative idea about the densification mechanisms in the two layers of different deformation behaviour. This can be studied in detail using quantitative metallographic techniques.

3) Further investigation can be done to tailor the CTE value of the Copper-Invar-Copper laminated strip to different levels by changing the Cu : Invar : Cu thickness ratio in the finished strip.

APPENDIX

1. Calculation of The Final Composition of MA Invar

The EMPA studies yielded the following composition of the MA Invar powder,

Constituent	Fe	Ni	W
wt.%	65.73	31.61	2.66

Now tungsten (W) is not present in the alloy as solid solution rather it is present as tungsten carbide (WC) and since wt.% carbon could not be arrived at from the EMPA studies so tungsten carbide content is extrapolated from the tungsten content by the equivalence method. This gave the final composition as,

Constituent	Fe	Ni	WC
wt.%	65.61	31.56	2.83

2. Calculation of Theoretical Density of Invar

The theoretical density of the MA Invar is calculated using the following formula,

$$\rho_0 = \frac{W_{Fe} + W_{Ni} + W_{WC}}{\frac{W_{Fe}}{\rho_{Fe}} + \frac{W_{Ni}}{\rho_{Ni}} + \frac{W_{WC}}{\rho_{WC}}} = \frac{\sum W_i}{\sum \frac{W_i}{\rho_i}}$$

where, ρ_0 = Theoretical density of Invar, W_i = Weight fraction of 'i' element and ρ_i = Theoretical density of 'i' element.

In the present calculation ρ_{Fe}, ρ_{Ni} and ρ_{WC} are taken to be 7.87, 8.90 and 15.77 g/cc respectively which yielded a theoretical density value of 8.29 g/cc. The respective W_i are calculated from the final composition of MA Invar.

3. Calculation of Theoretical Density of Cu-Invar-Cu Laminated Strip

The theoretical density of Copper-Invar-Copper laminated strip is calculated using the following formula,

$$\rho_L = t_{Inv.}.\rho_{Inv.} + t_{Cu}.\rho_{Cu} = \sum t_i.\rho_i$$

where, ρ_L = Theoretical density of the laminated strip, t_i = Total thickness fraction of the 'i' constituent and ρ_i = Theoretical density of the 'i' constituent.

Here, thickness fraction 't_i' is used in place of volume fraction since thickness fraction is directly proportional to the volume fraction when longitudinal cross-sectional area is the same as is the case in the present study. Now, using 8.96 and 8.29 g/cc for ρ_{Cu} and $\rho_{Inv.}$ respectively and taking Cu : Invar : Cu thickness ratio to be 15.5 : 69 : 15.5 , the theoretical density of the laminated is found out to be 8.50 g/cc.

4. Calculation of The Composite Mechanical Properties of Cu-Invar-Cu Laminated Strip

The composite mechanical properties of Cu-Invar-Cu laminated strip are calculated by using the rule of mixture. The formula used is,

$$P_M = t_{Inv.}.P_{Inv.} + t_{Cu}.P_{Cu} = \sum t_i.P_i$$

where, P_M = A particular mechanical property of the laminated strip, t_i = Total thickness fraction of the 'i' constituent and P_i = Corresponding mechanical property of the 'i' constituent.

Now, taking average thickness ratio of Cu : Invar : Cu to be 15.5 : 69 : 15.5 the tensile and 0.2% proof strength of the laminated strip is found out to be 480 MPa and 324 MPa respectively. The following property values are used in the above calculation,

Property	Copper	Invar
U.T.S (MPa)	235	590
0.2% Proof Strength (MPa)	93	428

REFERENCES

— [1] R. K. DUBE : *Int. Mat. Rev.*, 1990, **35**, (5), 253-291.

[2] RICHARD A. CAMPO : *Met. Prog.*, 1985, Aug., 23-27.

[3] W. BETTERIDGE : in *'Nickel and its alloys'*, 104; 1977, Plymouth, Macdonald & Evans.

[4] S. V. ILANGO : M.Tech. dissertation, Indian institute of Technology, Kanpur, 1986.

[5] A. F. MARSHALL : *Powder Metall.*, 1960, (5), 24-31.

[6] G. I. ASKENOV : *Sov. Powder Metall. Met. Ceram.*, 1970, **5**, (89), 370-374.

[7] E. B. LOZHECHNIKOV : *Sov. Powder Metall. Met. Ceram.*, 1976, **5**, (161), 339-342.

[8] A. M. MUSHIKHIN : *Sov. Powder Metall. Met. Ceram.*, 1978, **2**, (182), 87-90.

[9] M. R. DUSTOOR : *Met. Powder Rep.*, 1982, **37**, 92-93.

[10] D. H. RO and M. W. TOAZ : in *'Progress in powder metallurgy'*, vol.38, 311-338; 1982, NJ, Metal Powder Industries Federation. Cited in ref.[1].

[11] O. A. KATRUS and G. A. VINOGRADOV : *Sov. Powder Metall. Met. Ceram.*, 1962, **5**, (11), 357-362. Cited in ref.[1].

[12] M. L. MACKAY : *Met. Prog.*, 1977, **111**, (6), 32-35.

[13] E. J. HAYES and D. H. ANTONSEN : *Met. Powder Rep.*, 1984, **41**, 71-73.

[14] R. K. DUBE : *Int. Mat. Rev.*, 1990, **35**, (5), 261-262.

[15] RANDALL M. GERMAN : in *'Powder injection molding'*, 99-120; 1990, NJ, Metal Powder Industries Federation.

[16] G. Y. ONODA, Jr. : in *'Ceramic processing before firing'* (ed. G. Y. ONODA, Jr. and L. L. HENCH), 235-251; 1978, New York, Wiley.

[17] RANDALL M. GERMAN : in *'Powder injection molding'*, 440-443; 1990, NJ, Metal Powder Industries Federation.

[18] R. G. SWEET : U.K. Patent No.1115723, May 1968.

[19] R. K. DUBE : *Int. Mat. Rev.*, 1990, **35**, (5), 263-267.

[20] J. A. LUND : *J. Met.*, 1958, **10**, (11), 731-734.

[21] D. G. HUNT and R. EBORALL : *Powder Metall.*, 1960, (5), 1-23.

[22] J. DAVIES, W. M. GIBBON and A. G. HARRIS : *Powder Metall.*, 1968, **11**, 295-313.

[23] D. K. WORN and R. P. PERKS : *Powder Metall.*, 1959, (3), 45-71.

[24] G. M. STURGEON *et al.* : *Powder Metall.*, 1968, **11**, 314-329.

[25] C. H. WEAVER *et al.* : *Int. J. Powder Metall.*, 1972, **8**, 3-15.

[26] T. KIMURA *et al.* : *Rev. Electr. Commun. Lab.*(Jpn.), 1964, **12**, 341-354.

[27] M. D. AYERS : *Ind. Heat.*, 1974, **41**, (9), 22-25.

[28] P. H. WARREN and M. DONNELLY : *Powder Metall.*, 1984, **27**, 217-220.

[29] SAMUEL J. ROSENBERG : in *'Nickel and its alloys'*, 1968, 25-26 and 127-135, U.S. Dept. of Commerce, National Bureau of Standards.

[30] G. BÉRANGER, E. DUFFAUT, J. MORLET and J. F. TIERS (editors) : in *'The iron-nickel alloys'*, 34-38; 1996, Lavoisier Publishing.

[31] F. DUFFAUT and R. COZAR : in *'The iron-nickel alloys'* (edited by G. BÉRANGER *et al.*), 110-134; 1996, Lavoisier Publishing.

[32] BEN MOSTAPHA *et al.* : *Journal de Physique*, 1990, 51 sup.,**C1**, 445-450. Cited in ref.[30].

[33] CHARLES A. HARPER and RONALD M. SIMPSON (ed.) : in *'Electronic materials and process handbook'*, ch.11, 26-29, McGraw-Hill International.

[34] V. A. VERSHININ *et al.* : *'Sov. Powder Metall. Met. Ceram.*, 1990, **9**, (333), 757-758.

[35] V. A. VERSHININ *et al.* : *'Sov. Powder Metall. Met. Ceram.*, 1990, **1**, (349), 89-91.

[36] Tension Testing of Metallic Materials, E8-61T ASTM Standards, Part-3, 165; 1961, Philadelphia, American Society of Testing and Materials.

[37] C. E. GUILLAUME : *'C. R. Acad. Sc.'*, 1897, **124**, 176-179 and 752-755. Cited in ref.[30].

[38] R. K. DUBE and P. K. BAGDI : *'Met. Trans.'*, 1993, **24A**, 1753-1760.

[39] S. BHARGAVA and R. K. DUBE : *'Met. Trans.'*, 1988, **19A**, 1205-1211.